

James K. Mitchell Lecture

In situ soil testing: from mechanics to interpretation

Hai-Sui Yu

Nottingham Centre for Geomechanics, The University of Nottingham, UK

Keywords: in situ soil testing, mechanics, interpretation, analysis, strength, stiffness, state, clay, sand

ABSTRACT: This paper reviews and evaluates the current use of fundamental mechanics in developing rational interpretation methods for deriving soil properties from in situ test results. The focus is on some of the most widely used in situ test devices including cone penetrometers with and without pore pressure measurements (CPTU and CPT), self-boring and cone pressuremeters (SBPMT and CPMT), and flat dilatometers (DMT). In situ tests in both cohesive and frictional soils for measuring strength and stiffness properties, in situ state parameters, consolidation coefficients, stress history and in situ stresses are considered in detail.

1 INTRODUCTION

In his foreword to the Author's book 'Cavity Expansion Methods in Geomechanics' (Yu, 2000), Professor James K. Mitchell stated:

'The ability to treat the results of cone penetration and pressuremeter tests in sand and clay on a realistic theoretical basis enhances their value for site characterisation and determination of relevant soil mechanical properties'.

The preparation of this inaugural Mitchell Lecture therefore provides a good opportunity to conduct a brief review of the current use of both continuum and particle mechanics in the interpretation of in situ soil tests for measuring design parameters. Because of time and space constraints, the review will be selective, and is organised in terms of different in situ tests and their related interpretation methods. The focus will be on the interpretation of cone penetration tests (CPT/CPTU), self-boring and cone pressuremeter tests (SBPMT/CPMT) and flat dilatometer tests (DMT) that is based on a sound understanding of the mechanics of these tests. The selected topics cover more recent developments and, to some extent, also reflect the Author's own research interests in the area.

In situ testing serves a number of purposes in geotechnical engineering, which include (Ladd et al., 1977; Wroth, 1984; Jamiokowski et al., 1985):

- Site classification and soil profiling.
- Measurement of a specific property of the ground.
- Development of empirical rules for foundation design.
- Control of construction.
- Monitoring of performance and back analysis.

Whilst all these operations will benefit from a good understanding of the mechanics of in situ tests, it is essential if an accurate measurement of a specific property of the ground is to be made. This is because, unlike laboratory testing, in situ testing is generally an indirect technique as soil properties cannot be obtained directly from measured response without solving it as a boundary value problem.

In a most comprehensive review on the measurement of soil properties in situ, Mitchell et al. (1978) identified the following main reasons for the increased use of field testing:

- To determine properties of soils, such as continental shelf and sea floor sediments and sands, that cannot be easily sampled in the undisturbed state.
- To avoid some of the difficulties of laboratory testing, such as sample disturbance and the proper simulation of in situ stresses, temperature and chemical and biological environments.
- To test a volume of soil larger than can conveniently be tested in the laboratory.

- To increase the cost effectiveness of an exploration and testing programme.

However it has also long been realised (Wroth, 1984) that the interpretation of in situ tests is beset with difficulties especially if their results are needed to assess the stress-strain and strength characteristics of the tested soils. Jamiokowski (1988) highlighted the following difficulties that could form the major sources of uncertainty:

- 1) With the exception of the self-boring pressuremeter tests (SBPMT) and some geophysical tests, all other in situ tests represent complex boundary value problems rendering their theoretical interpretation very difficult.
- 2) The drainage conditions during in situ tests are usually poorly controlled and present the problem of determining whether the tests have been performed in undrained, drained or partially drained conditions.

- 3) Frequently, during the execution of in situ tests the soil involved is subjected to effective stress paths (ESP) which are very different from those representative of the relevant engineering problem. Hence, the measured soil stress-strain response is ESP dependent, and reflects its anisotropic and elastoplastic behaviour. This represents one of the most difficult problems when interpreting in situ test results.
- 4) Due to the highly pronounced nonlinear behaviour of all soils, even at small strains, it is difficult to link the stress-strain characteristics obtained from in situ tests to the stress or strain level relevant to the solution of the specific design problem.

Despite a large amount of empiricism and oversimplified assumptions involved with interpretation, in situ testing has and will continue to play a key role in the characterisation of natural soil deposits. Table 1 lists some of the fundamental soil properties that in situ testing can measure with a sound theoretical basis.

Table 1: Some current in situ testing capabilities for measuring soil properties

| Test | Measured properties | Selected references |
|---|--|--|
| Cone penetration tests (CPT/CPTU) | Soil profiling Stress history (OCR) Consolidation coefficient In situ state parameter for sand Undrained shear strength Hydrostatic pore pressure | Robertson (1986) Wroth (1984), Mayne (1993) Baligh and Levadoux (1986) Teh (1987) Been et al. (1987) Yu and Mitchell (1998) Lunne et al. (1997) |
| Self-boring pressuremeter tests (SBPMT) | Horizontal in situ stress Shear modulus Shear strength Stress-strain curve In situ state parameter for sand Consolidation coefficient Small strain stiffness | Jamiolkowski et al. (1985) Wroth (1982) Gibson and Anderson (1961) Hughes et al. (1977) Palmer (1972) Manassero (1989) Yu (1994, 1996, 2000) Clarke et al. (1979) Byrne et al. (1990) Jardine (1992) Fahey and Carter (1993) Bolton and Whittle (1999) |
| Cone pressuremeter tests (CPMT) | Horizontal in situ stress Shear modulus Shear strength In situ state parameter for sand | Houlsby and Withers (1988) Schnaid (1990) Yu (1990) Yu et al. (1996) |
| Flat dilatometer tests (DMT) | Soil profiling Horizontal in situ stress Stress history (OCR) Shear strength In situ state parameter for sand | Marchetti (1980) Mayne and Martin (1998) Finno (1993) Huang (1989) The present paper - Yu (2004) |

Given the interpretation of an in situ test requires the analysis of a corresponding boundary value problem, some simplifying assumptions will have to be made as in the case of solving any other boundary value problems. In particular, assumptions will have to be made with respect to the following three aspects:

- 1) Geometry and boundary conditions.
- 2) Soil behaviour.
- 3) Water drainage conditions.

2 SELF-BORING PRESSUREMETER TESTS IN CLAY

2.1 Overview

The self-boring pressuremeter (shown in Figure 1) has been established as one of the best in situ testing devices for measuring soil properties since its initial development over three decades ago in France (Baguelin et al., 1972) and the UK (Wroth and Hughes, 1972). Almost all the theoretical interpretation methods developed for it were based on the fundamental assumption that the pressuremeter geometry is such that the test can be simulated as the expansion and/or contraction of an infinitely long, cylindrical cavity in the soil. The advantage of this fundamental assumption is that the pressuremeter problem becomes one-dimensional for which many analytical solutions exist even for complex soil models (Yu, 2000). For tests in clay, it is often assumed that the test is carried out fast enough so that the undrained condition may be valid. With respect to soil behaviour, many models of various complexities (e.g., linear or nonlinear elastic together with perfectly plastic or strain hardening plastic models) have been used in the interpretation.

In recent years, the validity of these earlier assumptions with respect to pressuremeter geometry, water drainage and soil behaviour has been assessed in detail by numerical methods. It is now known that some of these simplifying assumptions could lead to significant errors in the derived soil properties.

2.2 Undrained shear strength

Self-boring pressuremeters are frequently used to determine undrained shear strengths of clays. Most interpretation methods take the following steps: First, a complete stress-strain relation is assumed for the soil, based on which the theoretical pressuremeter curves can be obtained by analysing the test as a cylindrical cavity expansion problem, either analytically or numerically. Then by matching some key or all parts of the theoretical pressuremeter curves with

those of a real pressuremeter test curve, the undrained shear strength may be estimated. Examples of the interpretation methods include Gibson and Anderson (1961), Jefferies (1988), and Yu and Collins (1998).

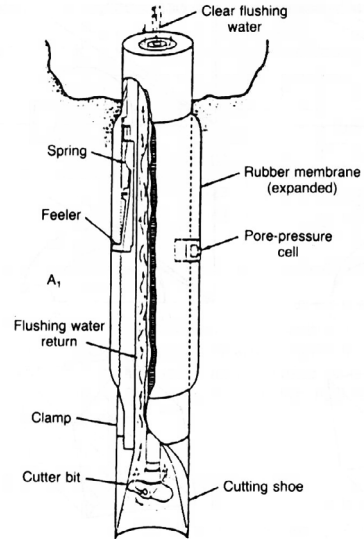


Figure 1: The Cambridge self-boring pressuremeter

2.2.1 Total stress loading analysis

Gibson and Anderson (1961) were among the first to use cavity expansion theory to develop interpretation methods for deriving soil properties from pressuremeter test results. In their analysis, the clay was assumed to behave as a linear elastic-perfectly plastic Tresca material obeying the following failure criterion:

$$\sigma_1 - \sigma_3 = 2S_u \quad (1)$$

where σ_1 and σ_3 are the major and minor principal stresses, and S_u is the undrained shear strength, whose value is not unique for a clay but depends on stress conditions imposed by a particular test (Wroth, 1984).

The pressuremeter test was idealised as the expansion of an infinitely long, cylindrical cavity in soil under undrained conditions. For simplicity, a total stress formulation was used in the analysis of Gibson and Anderson (1961). With the above assumptions, cavity expansion theory can be used to give the following theoretical pressuremeter expansion curve at the stage of plastic loading:

$$P = \sigma_{h0} + S_u \left\{ 1 + \ln \left(\frac{G}{S_u} \right) \right\} + S_u \ln \frac{\Delta V}{V} \quad (2)$$

where $\Delta V/V = (a^2 - a_0^2)/a^2$ is the volumetric strain; a and a_0 are the current and initial cavity radii respectively; P and σ_{h0} are the total pressuremeter pressure and total in situ horizontal stress; and G is the shear modulus of the soil.

The theoretical pressuremeter curve, as defined by equation (2), suggests that if pressuremeter results are plotted in terms of cavity pressure against the logarithm of the volumetric strain, the slope of the plastic portion (which is a straight line) is equal to the undrained shear strength of the soil S_u .

2.2.2 Total stress unloading analysis

Jefferies (1988) and Houlsby and Withers (1988) independently extended Gibson and Anderson's solution to include unloading. Jefferies (1988) derived the unloading solution for application to self-boring pressuremeter tests, where some small strain assumptions were used to simplify the mathematics. On the other hand, Houlsby and Withers (1988) were concerned with cone pressuremeter tests for which a large strain analysis is necessary.

The small strain cavity unloading solution, as derived by Jefferies (1988), can be expressed in the following form:

$$P = P_{\max} - 2S_u \left\{ 1 + \ln \left(\frac{G}{S_u} \right) \right\} - 2S_u \ln \left\{ \frac{a_{\max}}{a} - \frac{a}{a_{\max}} \right\} \quad (3)$$

where a_{\max} is the cavity radius at the end of the loading stage, P_{\max} is the cavity pressure at the end of the loading stage and a denotes cavity radius at any stage of pressuremeter unloading.

The theoretical pressuremeter unloading solution, as defined by equation (3), suggests that if the pressuremeter unloading results are presented as the pressuremeter pressure versus $-\ln(a_{\max}/a - a/a_{\max})$, the slope of the plastic unloading portion (which is a straight line) is equal to twice the soil undrained shear strength.

2.2.3 Total stress analysis with a hyperbolic soil model

If the stress-strain behaviour of clay can be described by a hyperbolic equation, then closed form solutions can be obtained for cavity expansion

curves if elastic strains are ignored (Prevost and Hoeg, 1975; Denby and Clough, 1980). Both strain hardening and strain softening may be considered. For example, in the case of strain hardening, the stress-strain relation may be described as follows:

$$q = \frac{\gamma}{D + \gamma} q_u \quad (4)$$

where q is defined as $\sqrt{3}/2$ times the difference of the major and minor principal stresses and γ is shear strain (i.e. the difference between the major and minor principal strains). D is a soil constant and the second soil constant q_u is the ultimate shear stress (i.e. $\sqrt{3}$ times the undrained shear strength). It then follows that the pressuremeter loading curve can be described as a function of two soil constants D and q_u in the following closed form:

$$P = \sigma_{h0} + \frac{q_u}{\sqrt{3}} \ln \left(1 + \frac{2}{\sqrt{3}D} \varepsilon_c \right) \quad (5)$$

where $\varepsilon_c = (a - a_0)/a_0$ is the cavity strain. In practice, the constant D may be easily chosen for a given soil. If this is the case, pressuremeter loading curves may be used to estimate the ultimate shear stress (strength). This can be achieved by plotting the pressuremeter loading results in terms of cavity pressure P versus $\ln \left(1 + \frac{2}{\sqrt{3}D} \varepsilon_c \right)$. The slope of the pressuremeter curve in this plot should be equal to the undrained shear strength S_u .

2.2.4 Effective stress analysis with critical state models

The self-boring pressuremeter test in clay is usually interpreted using undrained cavity expansion theory based on total stresses. This is reasonably accurate for normally and lightly overconsolidated clays where the shear resistance of the soil does not change significantly during the pressuremeter test. For heavily overconsolidated clay, however, the shear resistance may vary considerably with deformation history and this cannot be easily accounted for by the total stress approach with a perfectly plastic soil model.

Collins and Yu (1996) were the first to derive analytical solutions for large strain cavity expansion in critical state soils. Using these analytical solutions, Yu and Collins (1998) showed that the direct application of the total stress-based interpretation method of Gibson and Anderson (1961) is accurate

for soils with low overconsolidation ratio (*OCR*) values. However the total stress approach tends to underestimate undrained shear strength of the soil for heavily overconsolidated soils. As shown in Figure 2, the underestimate could be as high as 50% for soils with a very high *OCR* value. A more detailed discussion can be found in Yu and Collins (1998) and Yu (2000).

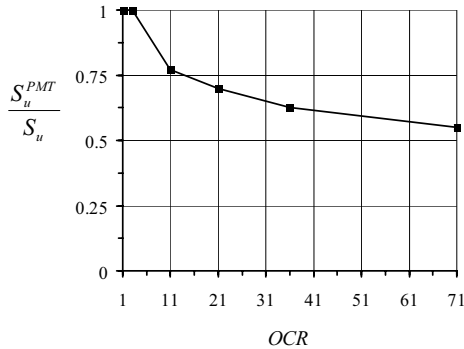


Figure 2: Ratio of pressuremeter strength S_u^{PMT} to triaxial strength S_u versus *OCR* (after Yu and Collins, 1998)

2.3 Complete shear stress-strain curve

The development of a method for deducing a complete shear stress-strain curve from measured pressuremeter expansion results was generally attributed to Palmer (1972), Baguelin et al. (1972) and Ladanyi (1972). As noted by Hill (1950), however, the same procedure for deriving shear stress-strain relation from a known cavity expansion curve had been outlined many years earlier by W.M. Shepherd, as reported in Morrison (1948). The key feature of this alternative approach lies on the fact that there is no need to assume a specific form of stress-strain relations apart from a plastic flow rule (i.e., incompressibility for undrained loading).

It can be shown (Yu, 2000) that the shear stress definition and the incompressibility condition lead to the following cavity expansion curve:

$$P = \sigma_{h0} + \int_0^{\epsilon_c} \frac{\tau}{\epsilon} d\epsilon \quad (6)$$

where ϵ_c is the cavity strain and τ is shear stress. The above equation can be used to derive the following shear stress-strain relation:

$$\tau = \epsilon_c \frac{dP}{d\epsilon_c} \quad (7)$$

in which the derivative $dP/d\epsilon_c$ is readily obtained from the measured pressuremeter results in terms of P versus ϵ_c .

It has now been recognised that a serious limitation of this method is that the derived stress-strain curve appears to be very sensitive to initial disturbance and the datum selected for the strain (Wroth, 1984; Mair and Wood, 1987).

2.4 Consolidation coefficients

Another soil property that can be measured with a self-boring pressuremeter is the horizontal consolidation coefficient c_h . Such a measurement can be made by conducting either a 'strain holding test' (Clarke et al., 1979) or a 'pressure holding test' (Fahy and Carter, 1986).

When a pressuremeter is expanded in clay under undrained conditions, excess pore pressures are generated in the surrounding soil which is deformed plastically. If at this stage the diameter of the pressuremeter is held constant, relaxation of soil is observed by the decrease of the measured excess pore pressure and the total cavity pressure. This is called a strain-holding test. On the other hand, if the total pressure is held constant, relaxation occurs as the decrease of the measured excess pore pressure and the continuing increase in cavity diameter. This is called a pressure-holding test.

If the pressuremeter expansion is modelled as a cylindrical cavity expansion process in a Tresca soil, then it can be shown (Gibson and Anderson, 1961) that the excess pore pressure takes a maximum at the cavity wall, which is linked to the cavity volumetric strain by

$$\Delta U_{\max} = S_u \ln\left(\frac{G}{S_u}\right) + S_u \ln\left(\frac{\Delta V}{V}\right) \quad (8)$$

If the cavity radius is held constant (i.e., strain holding test), the excess pore pressure dissipates. The consolidation coefficient may be estimated using a dimensional time factor $T_{50} = c_h t_{50}/a^2$, where t_{50} is the time taken for the excess pore pressure to fall to half its maximum value.

By assuming that soil behaves as an entirely elastic material during consolidation, a closed form solution for the time dependence of the excess pore pressures around a cavity was derived by Randolph and Wroth (1979). A subsequent elastoplastic consolidation analysis carried out by Carter et al. (1979) using the finite element method confirmed that the elastic consolidation analysis of Randolph and Wroth (1979) is sufficiently accurate. In particular, a rela-

relationship between the normalised maximum excess pore pressure $\Delta U_{\max}/S_u$ and the time factor T_{50} was obtained and is plotted in Figure 3.

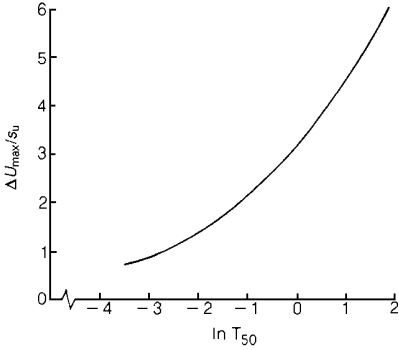


Figure 3: Time for 50% pore pressure decay at the cavity wall (after Randolph and Wroth, 1979)

It then follows that with the actual time t_{50} and the normalised maximum excess pore pressure at the cavity wall measured in pressuremeter strain-holding tests, the correlation, as shown in Figure 3, can be used to determine the horizontal consolidation coefficient c_h .

2.5 Shear modulus and non-linear stiffness

Wroth (1982) noted that a major use of the self-boring pressuremeter is to measure soil stiffness. As stressed by Jamiolkowski et al. (1985) and Mair and Wood (1987), the measurements obtained at the initial stage of a pressuremeter expansion test are not usually reliable. Therefore emphasis is more often placed on using small unloading-reloading loops at later stages of the tests for estimating soil stiffness. For a linear-elastic/plastic soil, cylindrical cavity expansion theory suggests that the shear modulus of the soil is equal to half the slope of an unloading-reloading loop of a pressuremeter curve. However it is well known that soil behaviour is often highly nonlinear even at small strains (e.g., Burland, 1989). In other words, the secant shear modulus of a soil is the highest at very small strains and tends to decrease considerably with increasing shear strain.

If the soil being tested is linear-elastic/plastic then in theory the unloading curve should coincide with reloading curve for a pressuremeter unloading-reloading loop. The slope of such an elastic pressuremeter loop is twice the shear modulus of the soil. Otherwise the small strain behaviour of the soil would be nonlinear and in this case, the interpretation of the pressuremeter results would be more

complex because of the strain dependence of the stiffness (Jardine, 1992). For a nonlinear-elastic stress-strain behaviour, a number of theories can be used to describe it. Simple and well-known examples include those based on a power law (Bolton and Whittle, 1999) and a hyperbolic equation (Denby and Clough, 1980).

If an elastic soil stress-strain relationship can be described by the following power law:

$$\tau = G_l \gamma^\beta \quad (9)$$

where τ is the shear stress (i.e. half of the difference between the major and minor principal stresses) and γ is the shear strain. G_l and β are two nonlinear elastic constants and the value of β is between 0 and 1. Obviously G_l is the shear modulus for a linear elastic material when $\beta = 1$. It would be useful if we could derive the soil constants G_l and β from pressuremeter test results.

Cavity expansion theory suggests that for an elastic material governed by equation (9), the following initial elastic cavity stress-strain relation from rest may be derived (Ladanyi and Johnston, 1974; Bolton and Whittle, 1999):

$$P = P_0 + \frac{G_l}{\beta} \gamma_c^\beta \quad (10a)$$

or

$$\ln(P - P_0) = \ln\left(\frac{G_l}{\beta}\right) + \beta \ln(\gamma_c) \quad (10b)$$

where the shear strain at the cavity wall is defined as $\gamma_c = 2 \ln(a/a_0)$ with a and a_0 being the current and initial cavity radii respectively. P and P_0 are the current and initial cavity pressures respectively.

Now consider the case when the cavity pressure has increased to a value say, P_{\max} , then it is gradually reduced. In this case (i.e., pressuremeter unloading), we can derive the following theoretical relationship between cavity pressure and contraction (note the initial condition is at the end of cavity loading test):

$$P = P_{\max} - \frac{G_l}{\beta} \gamma_c^\beta \quad (11a)$$

or

$$\ln(P_{\max} - P) = \ln\left(\frac{G_l}{\beta}\right) + \beta \ln(\gamma_c) \quad (11b)$$

where the shear strain at the cavity wall is defined as $\gamma_c = 2 \ln(a_{\max}/a)$ with a and a_{\max} being the current

and maximum cavity radius at the end of the loading stage respectively.

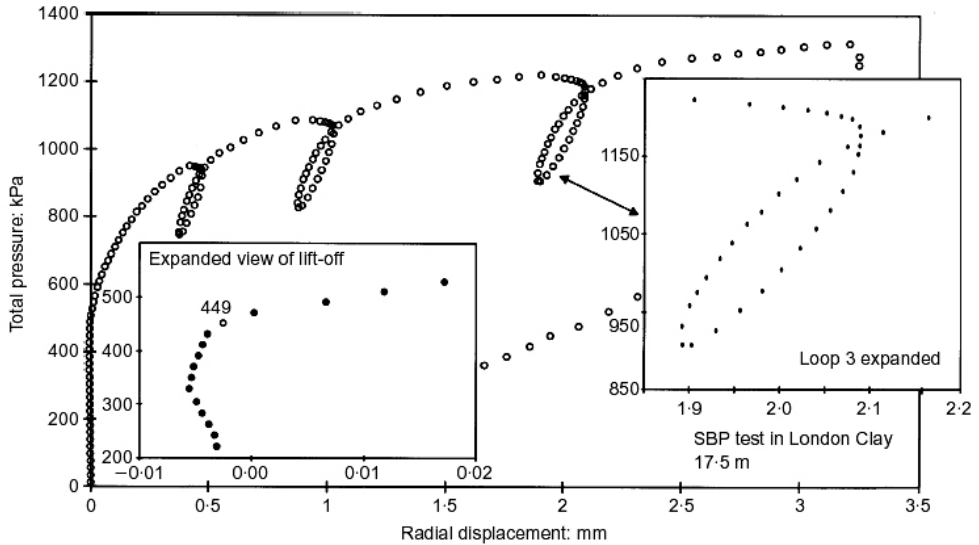


Figure 4: A self-boring pressuremeter test in London clay with three unloading-reloading loops (after Bolton and Whittle, 1999)

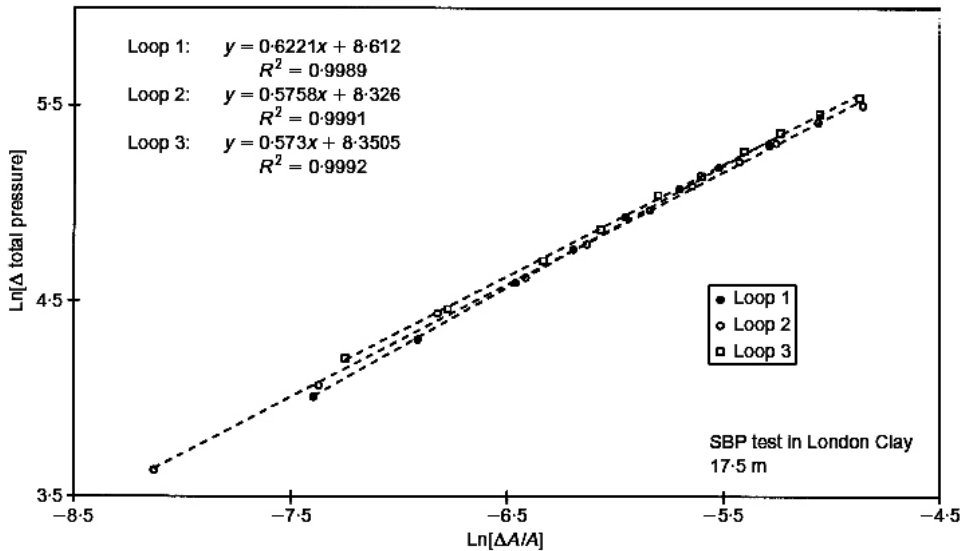


Figure 5: Deriving the nonlinear elastic relationship from unloading-reloading loops (after Bolton and Whittle, 1999)

Equation (11b) suggests that if the pressuremeter unloading results are plotted in terms of $\ln(P_{\max} - P)$ versus $\ln(\gamma_c) = \ln(2(\epsilon_c)_{\max} - 2\epsilon_c)$, then the slope is equal to the nonlinear constant β . The other nonlinear elastic constant G_I can be derived from the fact

that the intercept of the plot is equal to $\ln(G_I/\beta)$. Figure 4 shows the results of a self-boring pressuremeter test in London clay with three unloading/reloading loops. By using equation (10b), Bolton and Whittle (1999) suggested a similar method that

can be used to derive the elastic constants G_i and β (as shown in Figure 5).

Alternatively, a nonlinear-elastic stress-strain relation may be described by a hyperbolic relation of the following type:

$$\tau = \frac{\gamma}{1/G_i + \gamma/\tau_{\max}} \quad (12)$$

where again two material constants are required. They are the initial shear modulus G_i and the maximum shear stress τ_{\max} at infinite shear strain.

Using the stress-strain relation (12), cavity expansion theory can be used to give the following theoretical cavity contraction curve for elastic pressuremeter unloading:

$$P = P_{\max} - \tau_{\max} \ln \left(1 + \frac{G_i}{\tau_{\max}} \gamma_c \right) \quad (13)$$

Although not as easy to use as equation (11b), equation (13) may also be used to match a measured pressuremeter unloading curve in order to estimate the nonlinear elastic constants G_i and τ_{\max} (e.g., Ferreira and Robertson, 1992).

2.6 Sources of inaccuracy

The interpretation methods described in the preceding sections were developed based on simplified assumptions about pressuremeter geometry, water drainage and initial disturbance. Possible inaccuracies of soil properties caused by these assumptions can be assessed numerically.

2.6.1 Effect of finite pressuremeter length

All the interpretation methods described so far were based on the fundamental assumption that the pressuremeter is sufficiently long so that its expansion can be simulated as the expansion of an infinitely long, cylindrical cavity. In reality, however, the pressuremeter length varies depending on the type of pressuremeter used. A typical example of a pressuremeter is the Cambridge self-boring pressuremeter which had a length to diameter ratio of 6. It is therefore necessary to use numerical methods (such as finite elements) to assess the validity of using one-dimensional cavity expansion analysis to solve the two-dimensional pressuremeter problem. Research in this area was first undertaken by Yu (1990, 1993a) and Yeung and Carter (1990), who were later followed by many other researchers.

The most important conclusion of these numerical studies was that ignoring the two-dimensional

pressuremeter geometry would significantly overestimate the undrained shear strength. For example, by using a linear elastic perfectly plastic model obeying the von Mises failure criterion, Yu (1990, 1993a) obtained the following correction factor:

$$F_c = \frac{S_u}{S_u^6} = 1 - 0.02 \ln \left(\frac{G}{S_u^6} \right) \quad (14)$$

where S_u^6 is the undrained shear strength derived from pressuremeters with a length to diameter ratio of 6 (as for the Cambridge self-boring pressuremeter). The actual undrained shear strength can then be estimated by multiplying the undrained shear strength S_u^6 by a reduction factor F_c given by equation (14). A more recent study of the pressuremeter geometry effect, reported by Yu et al. (2003) using a critical state model, suggests that effective stress analysis gives a smaller geometry effect. In addition, the effect is found to decrease with the *OCR* value of the soil.

It was also found that the two-dimensional pressuremeter geometry has a quite small effect on the measurement of stiffness (Houlsby and Carter, 1993) and consolidation coefficients (Jang et al., 2003).

2.6.2 Effect of partial drainage and strain rate

The validity of the undrained assumption for pressuremeter analysis in clay has been assessed by Fioravante et al. (1994) and Jang et al. (2003) amongst others. These studies indicate that the pressuremeter expansion can be assumed to occur under the undrained condition at a 1%/min rate, only if the coefficient of permeability of the clay is less than 10^{-9} m/s . Otherwise the effect of partial drainage would become significant and the undrained condition is no longer a valid assumption.

The effect of strain rate on pressuremeter test results was investigated in detail by Pyrah and Anderson (1990) and Prapaharan et al. (1989). From a parametric study in the latter paper, it was concluded that if laboratory results at a strain rate of 0.01%/min are the reference, then the usual pressuremeter test gives an overestimate of the undrained shear strength. The strain rate effects are most significant for soils with a strain softening behaviour. For a strain hardening soil, the pressuremeter test can yield a derived stress-strain curve similar to that of a material curve corresponding to the reference strain rate.

2.6.3 Effect of disturbance during pressuremeter installation

Although it was commonly assumed that the installation of a self-boring pressuremeter causes no disturbance to the surrounding soil, in reality some disturbance would inevitably occur. As mentioned earlier, the method for deriving stress-strain relations from pressuremeter curves is particularly sensitive to initial disturbance.

A theoretical study of the possible effects of initial disturbance has been reported by Aubeny et al. (2000) using strain path analysis. This study indicates that disturbance induced during ideal self-boring penetration (i.e., where the volume of soil extracted exactly balances the volume of soil displaced by the device) causes a reduction in lift-off pressures compared to the in situ horizontal stress and a higher peak undrained shear strength. The analysis also shows that more reliable undrained shear strengths can be derived from pressuremeter unloading tests.

3 SELF-BORING PRESSUREMETER TESTS IN SAND

3.1 Overview

As in clay, cavity expansion theory forms the main theoretical basis for the interpretation of self-boring pressuremeter tests in sand. For simplicity, the tests are assumed to be carried out under a fully drained condition so that excess pore pressures will be zero throughout the test. The main difference in behaviour between clay and sand lies in the significant volume change occurred in sand during shear, and this must be captured by any realistic sand model. Over the last two decades, significant advances have been made in the analysis of pressuremeter tests in sand using realistic stress-strain equations of various complexities (Yu, 2000).

3.2 Drained shear strength

Hughes et al. (1977) modified the analysis of Gibson and Anderson (1961) to account for the effect of dilation during drained pressuremeter tests in sand. To derive a closed form solution, they assumed that the angles of friction and dilation were constant during the pressuremeter test. From the analysis, a simple procedure was suggested for deriving the value of friction and dilation angles from the pressuremeter loading results. Subsequently an interesting drained analysis, similar to that of Palmer's undrained analysis in clay, has been proposed by Manassero (1989). With this analysis, a stress-strain relationship can be derived from the pressuremeter loading results provided that a plastic flow rule is assumed.

3.2.1 Angles of friction and dilation

Hughes et al. (1977) developed a small strain cavity expansion solution that can be used to deduce the angles of friction and dilation from the pressuremeter loading test results. In their analysis, the sand was assumed to behave as an elastic-perfectly plastic Mohr-Coulomb material obeying the following failure criterion in terms of effective stresses:

$$\frac{\sigma'_1}{\sigma'_3} = \frac{1 + \sin \phi}{1 - \sin \phi} \quad (15)$$

where ϕ is the angle of internal soil friction, which, like the undrained shear strength of clay, also depends on stress conditions imposed by a particular test (Wroth, 1984). By ignoring elastic deformation in the plastically deforming zone, the analytical solution for the cavity expansion curve in the plastic range can be approximated as follows:

$$\ln(P') = s \ln \varepsilon_c + A \quad (16)$$

where P' is the effective cavity pressure, $s = (1 + \sin \psi) \sin \phi / (1 + \sin \phi)$, A is a constant and ψ is the angle of soil dilation.

The theoretical pressuremeter loading curve, as defined by equation (16), indicates that if the pressuremeter results are plotted as the effective cavity pressure P' versus the cavity strain on a logarithmic scale, the slope of the plastic portion (which is a straight line) is equal to s , which is a function of the friction angle ϕ and dilation angle ψ . If Rowe's stress-dilatancy equation is used to link the angles of friction and dilation, we can obtain the following formula for deducing them from the pressuremeter loading slope and the angle of soil friction at the critical state ϕ_{cs} :

$$\sin \phi = \frac{s}{1 + (s-1) \sin \phi_{cs}} \quad (17)$$

$$\sin \psi = s + (s-1) \sin \phi_{cs} \quad (18)$$

3.2.2 Complete stress-strain curve

As shown by Manassero (1989) and Sousa Coutinho (1989), a pressuremeter loading curve can also be used to deduce a complete soil stress-strain curve, provided that a plastic flow rule can be assumed.

For dilatant sand, the relationship between the radial and hoop strains may be assumed to be related by an unknown function f such as $\varepsilon_r = f(\varepsilon_\theta)$ with a condition that $\varepsilon_r = 0$ when $\varepsilon_\theta = 0$. The function f must be determined numerically from the pres-

suremeter loading test results. Yu (2000) shows that the equations of equilibrium, strain compatibility condition and Rowe's stress-dilatancy relation can be combined to give the following equation:

$$1 + \frac{f'}{K} = -\frac{1}{\sigma'_r} \times \frac{d\sigma'_r}{d\varepsilon_\theta} \quad (19)$$

in which $K = (1 + \sin \phi_{cs}) / (1 - \sin \phi_{cs})$ and $f' = d\varepsilon_r / d\varepsilon_\theta$. The above equation cannot be integrated analytically. However when applying it at the cavity wall, the finite difference method can be used to solve for a numerical function f and therefore the relationship between the radial and hoop strains. This is possible because at the cavity wall both the effective radial stress σ'_r and $d\sigma'_r / d\varepsilon_\theta$ are given from the pressuremeter curve. The stress ratio is linked to the function f as follows:

$$\frac{\sigma'_r}{\sigma'_\theta} = -\frac{K}{f'} \quad (20)$$

Further application and extension of this approach were given by Ajalloeian and Yu (1998) and Silvestri (2001). Presented in Figure 6 are derived stress ratio-shear strain curves using this approach from the results of model pressuremeter tests in a large chamber obtained by Ajalloeian and Yu (1998) with three different pressuremeter length to diameter (L/D) ratios.

It is stressed that the above analysis is valid only when elastic deformation can be ignored in the plastically deforming zone. As will be discussed later, this assumption could have a significant effect on the derived soil strength properties (Yu, 1990).

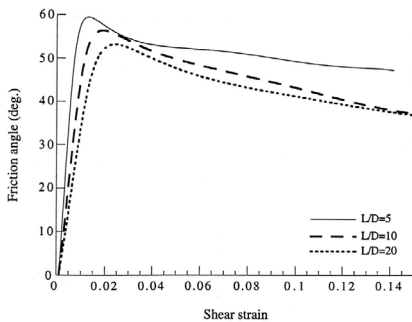


Figure 6: Derived stress ratio-shear strain curves from laboratory pressuremeter tests (after Ajalloeian and Yu, 1998)

3.3 In situ state parameter

A state parameter (defined as the vertical distance between the current state and the critical state line in the usual $v - \ln p'$ plot) was introduced by Wroth and Bassett (1965) and Been and Jefferies (1985) to combine the effects of both relative density and stress level on soil behaviour in a rational way. The state parameter concept represents an important step forward from the conventional relative density concept in characterising sand behaviour. It has been demonstrated that many commonly used sand properties, such as the angles of friction and dilation, normalise well to the state parameter. The practical application of the state parameter concept is dependent upon the ability to measure it in situ. To meet this demand, Yu (1994,1996) developed a procedure to deduce the in situ (or pre-shear) state parameter from either loading or unloading curves of a self-boring pressuremeter test in sand.

3.3.1 State parameter from loading results

Using a state parameter-based critical state soil model, Yu (1994) developed an interpretation method by which the results of a self-boring pressuremeter test can be correlated with the in situ sand state parameter. It was found that for a particular sand, a linear correlation exists between the pressuremeter loading slope s and the pre-shear (or in situ) state parameter of the soil. In addition, this correlation was found to be largely independent of initial stress state and soil stiffness, and may therefore be considered to be unique for a given soil.

The numerical results obtained for six different sands suggest that the following linear correlation may be used for practical purposes:

$$\xi_0 = 0.59 - 1.85s \quad (21)$$

where ξ_0 is the in situ sand state parameter and s is the measured pressuremeter loading slope. Once the state parameter is known, the angles of friction in situ can then be estimated using an average correlation between the angle of friction and state parameter (Been et al., 1987).

The validity of Yu's analysis was further confirmed by Hsieh et al. (2002) using the more advanced sand model MIT-S1.

3.3.2 State parameter from unloading results

As pointed out by Jamiolkowski et al. (1985), soil disturbance during the installation of a self-boring pressuremeter may have a significant effect on the shape of the initial loading portion of the pressuremeter curve. It is therefore necessary, whenever pos-

sible, to place less reliance on interpretation methods that are purely based on the initial portion of the test results.

Thus Yu (1996) developed an interpretation method for the unloading stage of a pressuremeter test in terms of the state parameter. The method uses the unloading pressuremeter curve to deduce the in situ state parameter, and thus represents an attractive alternative to the loading analysis. Using this unloading analysis, the pressuremeter results are plotted as $\ln(P')$ versus $-\ln((\varepsilon_c)_{\max} - \varepsilon_c)$, and the slope of the pressuremeter unloading curve s_d in this plot is then estimated. The numerical study with six different sands again confirms that there is a largely unique correlation between in situ state parameter and pressuremeter unloading slope, that is given by

$$\xi_0 = 0.53 - 0.33s_d \quad (22)$$

3.4 Shear modulus and small strain stiffness

Because of sampling difficulties, one of the most common uses of self-boring pressuremeter tests in sand is for the measurement of shear modulus (Wroth, 1982). However the interpretation and application of the soil stiffness derived from the pressuremeter unloading-reloading loops requires special care, and this is largely due to the strong dependence of soil stiffness on both stresses and strains (Bellotti et al., 1989).

3.4.1 Interpretation of unloading-reloading shear modulus

If the soil is linear elastic and plastic, then cavity expansion theory would suggest that the unloading-reloading loop of a pressuremeter test should be a straight line. The slope of the loop is twice the shear modulus of the tested soil. In reality, however, most soils exhibit a nonlinear elastic stress-strain feature even at very small strains. Therefore actual pressuremeter unloading and reloading sections do not coincide. Nevertheless some average slope of the loop is still widely measured to give the so-called pressuremeter unloading-reloading shear modulus G_{ur} , which may be regarded as a secant shear modulus for a nonlinear soil.

For a rational interpretation of soil moduli, it is crucial to note the fact that they are dependent on both stress and strain levels. Given that the stress level at which the unloading-reloading modulus is measured is different from that of an in situ state (i.e. a pre-shear state), it is useful to estimate the equivalent in situ shear modulus G_{ur}^i , at a particular

shear strain level (as represented by the size of the unloading-reloading cycle performed). A simple equation that can be used for this estimation is:

$$G_{ur}^i = G_{ur} \left(\frac{p'_0}{p'_m} \right)^n \quad (23)$$

where p'_0 and p'_m are the in situ mean effective stress and the mean effective stress at the cavity wall when the unloading-reloading cycle is performed. For sand, the value of n is generally in the range of 0.4-0.5, with a tendency to increase with increasing level of strains (Wroth et al., 1979).

3.4.2 Estimate of small strain (or maximum) shear modulus

At very small strains (say less than $10^{-4}\%$), the soil modulus is at peak and tends to decrease with increasing strain levels. This peak modulus is often termed as the maximum or small strain shear modulus G_0 . Unfortunately the small strain modulus is not a constant for a given soil and rather it is a function of the void ratio, mean stress level as well as stress ratios (Hardin, 1978; Yu and Richart, 1984). The following equation has been frequently used to describe this dependence (Hardin, 1978):

$$\frac{G_0}{p_a} = BF(e) \left(\frac{p'_m}{p_a} \right)^{0.5} (1 - 0.3k^{1.5}) \quad (24)$$

where p_a is the atmospheric pressure used as a reference pressure. p'_m is the effective mean stress and the stress ratio effect is expressed in terms of $k = (\sigma'_1/\sigma'_3 - 1)/[(\sigma'_1/\sigma'_3)_{\max} - 1]$. The parameters B and $F(e)$ depend on particle shape and void ratio e . Equation (24) has been shown to be in agreement with quality laboratory measurement of the small strain modulus such as those obtained using resonant column tests reported by Byrne et al. (1990).

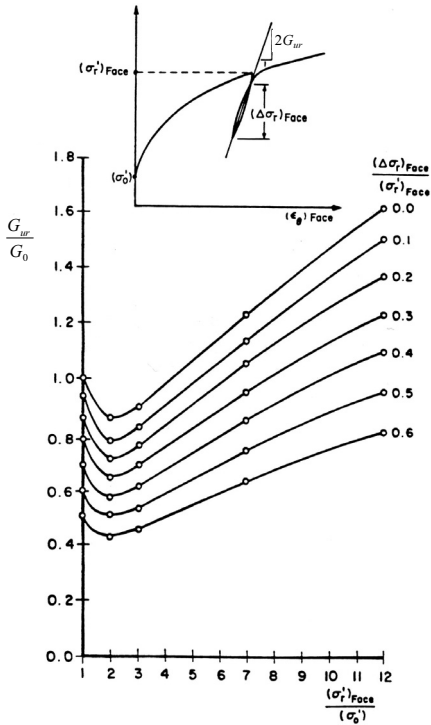


Figure 7: A chart for determination of G_0 from measured G_{ur} (after Byrne et al., 1990)

- 1) An elastic-plastic cavity expansion analysis to determine the stress field and volume change caused by pressuremeter expansion. These stresses allow the in situ small strain modulus values to be computed prior to pressuremeter unloading tests using equation (24).
- 2) A nonlinear elastic analysis to determine the displacement at the pressuremeter face upon unloading. These displacements are used to compute the equivalent elastic pressuremeter unloading-reloading shear modulus G_{ur} .
- 3) By comparing the unloading-reloading shear modulus with the in situ small strain shear modulus for various levels of applied cavity stress prior to unloading, and for various amounts of unloading, a chart is generated from which the ratio of G_{ur}/G_0 can be obtained depending on the applied pressuremeter loading and unloading conditions.

Figure 7 presents such a chart developed by Byrne et al. (1990) for determining the in situ small strain shear modulus from a pressuremeter unloading-reloading modulus. A further study has been presented by Fahey and Carter (1993).

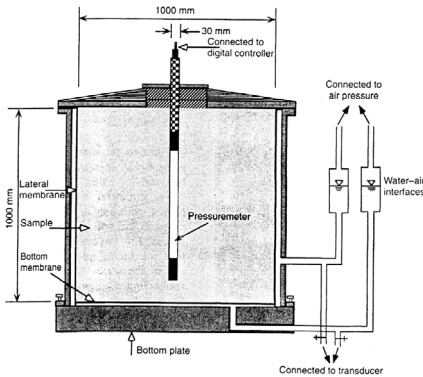


Figure 8: The chamber used by Ajalloeian and Yu (1998)

To derive the small strain shear modulus G_0 , Byrne et al. (1990) proposed a numerical procedure to correlate it with the pressuremeter unloading-reloading modulus. The procedure takes the following steps:

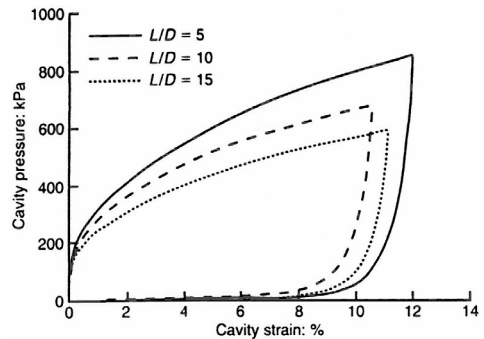


Figure 9: Laboratory results of finite pressuremeter length effects (after Ajalloeian and Yu, 1998)

3.5 Sources of inaccuracy

As in the case for tests in clay, the possible effects of the simplified assumptions used in developing the above mentioned interpretation methods can be assessed either using numerical methods and/or more realistic soil models.

3.5.1 Effect of finite pressuremeter length

The effect of ignoring the finite pressuremeter length on drained pressuremeter analysis was assessed in detail by Yu (1990) using finite element methods. The result of this numerical study was confirmed by a comprehensive chamber study of finite pressuremeter length effects reported by Ajalloeian and Yu (1998) – see Figures 8 and 9.

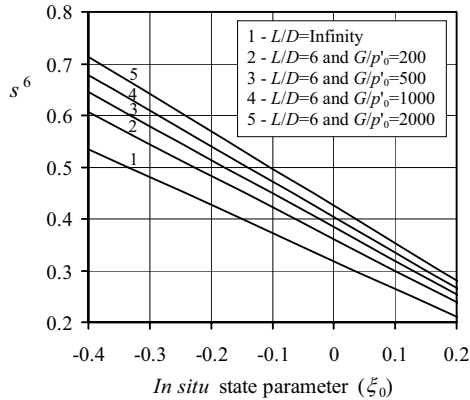


Figure 10: A chart to derive in situ state parameter by accounting for the effect of finite pressuremeter length

As expected, both numerical and laboratory chamber studies suggest that a finite pressuremeter length results in a stiffer pressuremeter loading response. In particular, the pressuremeter loading slope s^6 for a length to diameter ratio of 6 was found to be 10-20% higher than those from the cylindrical cavity expansion theory. The overestimate is slightly dependent upon the soil stiffness index (defined as the shear modulus G over the initial mean effective stress, p'_0), as given by the following equation:

$$F_c = \frac{s}{s^6} = 1.19 - 0.058 \ln \left(\frac{G}{p'_0} \right) \leq 1 \quad (25)$$

In practice, the effect of finite pressuremeter length can be simply taken into account by determining the correction factor F_c from equation (25). This can then be applied to the measured pressuremeter loading slope before correlating with soil properties such as the angles of friction and dilation (equations (17) and (18)) and the in situ state parameter (equation (21)). Figure 10 presents a chart that can be used to derive in situ state parameter from the pressuremeter loading results by accounting for the effect of finite pressuremeter length.

The experimental data obtained by Ajalloeian and Yu (1998) suggests that finite pressuremeter length has a smaller effect on unloading results than on the loading section of the test. This is to be expected since the unloading involves a very small cavity contraction.

3.5.2 Effect of elastic deformation in the plastically deforming zone

It was noted earlier that elastic deformation in a plastically deforming region was ignored by both Hughes et al. (1977) and Manassero (1989). The effect of this simplifying assumption was assessed by Yu (1990). It was shown that neglecting elastic strain in plastic zones tends to give a softer pressuremeter response, and therefore underestimates the measured angle of friction. The study also suggests that the effect of elastic deformation in the plastic zone is particularly marked for dense soil with a high stiffness index. Using a numerical study, Yu (1990, 1993a) suggested the following single equation for the corrected angle of friction ϕ^c to account for the effect of both finite pressuremeter length and elastic deformation in the plastically deforming zone:

$$\frac{\phi^c}{\phi^e} = 1.36 - 0.078 \ln \left(\frac{1 - \sin \phi^e}{\sin \phi^e} \times \frac{G}{\sigma'_{\theta 0}} \right) \quad (26)$$

where ϕ^e is the friction angle derived from the method of Hughes et al. (1977) for pressuremeters with a length to diameter ratio of 6.

3.5.3 Effect of sand particle crushing

It is now established that sand particles crush at high stresses (McDowell and Bolton, 1998). One important feature common to all the findings of recent studies in this area is the distinct steepening of the compression line at elevated stresses (Konrad, 1998).

The possible effect of particle crushing on cavity expansion solutions in sands was studied recently by Russell and Khalili (2002). In their work, a single function for a nonlinear critical state line was introduced which is able to capture the main features of sand behaviour for stresses that are lower and higher than those needed for particle crushing. Limited pressuremeter expansion calculations given by Russell and Khalili show that ignoring particle crushing may lead to a stiffer pressuremeter loading response. This would be particularly true for tests performed in sands with high initial density and/or mean effective stresses.

4 CONE PENETRATION TESTS IN CLAY

4.1 Overview

Over the last few decades, cone penetration testing (with or without pore pressure measurement, CPTU/CPT) has been established as the most widely used in situ testing device for obtaining soil profiles worldwide. This has been achieved mainly by developing empirical correlations and soil classification charts (Robertson, 1986; Lunne et al., 1997; Mitchell and Brandon, 1998). In addition, good progress has also been made, though slowly, in the understanding of the fundamental mechanics of the cone penetration tests in undrained clay. This progress provides confidence in derived soil properties from CPTU test results. Yu and Mitchell (1996, 1998) noted the great difficulties of carrying out a rigorous analysis of cone penetration problems and gave a brief review and evaluation of the theoretical methods that may be used for such an analysis. The most widely used theories are:

- 1) Bearing capacity methods (BCM)
- 2) Cavity expansion methods (CEM)
- 3) Strain path methods (SPM)
- 4) Finite element methods (FEM)

While each of these four theories may be used alone for cone penetration analysis (Yu and Mitchell, 1996, 1998), better predictions of the cone penetration mechanism may be achieved if some of them are used in combination. Successful examples are SPM-FEM (Teh and Houlsby, 1991), CEM-SPM (Yu and Whittle, 1999), CEM-FEM (Abu-Farsakh et al., 2003), and CEM-BCM (Salgado et al., 1997).

Apart from the above theories that have been the main approaches currently used for cone penetration analysis, other methods such as the discrete element method (DEM) may also be useful for cone penetration analysis in granular materials (e.g., Huang and Ma, 1994; Yu et al., 2004).

4.2 Undrained shear strength

If cone penetration tests in clay are assumed to occur under undrained conditions, cone tip resistance q_c (with the correction for porewater effects on the back of the cone tip) may be related to the undrained shear strength S_u as follows:

$$q_c = N_c S_u + \sigma_0 \Rightarrow S_u = \frac{q_c - \sigma_0}{N_c} \quad (27)$$

where σ_0 denotes the in situ total stress (either vertical or mean total stress depending on the type of theory used for cone penetration analysis). The theory of cone penetration can be used to give the so-called cone factor N_c .

4.2.1 Cavity expansion combined with steady penetration of infinite cone

Based on the rigorous plasticity solutions of steady penetration of a rigid cone in a von Mises soil (Durban and Fleck, 1992; Sagaseta and Houlsby, 1992), Yu (1993b) derived the following expression for the cone factor:

$$N_c = \frac{2}{\sqrt{3}} \left[\pi + \alpha + \arcsin(\lambda_c) + \lambda_c \cot \frac{\alpha}{2} - \sqrt{1 - \lambda_c^2} + \frac{H}{2} \right] + \frac{2}{\sqrt{3}} \ln \left(\frac{\sqrt{3}}{2} I_r \right) \quad (28)$$

where $I_r = G/S_u$ is known as the rigidity or stiffness index and the parameter H is defined as

$$H = \frac{\sin \frac{\beta}{2} + \lambda_c \sin \beta}{\cos \frac{\beta}{2} - \cos \beta}; \quad \beta = 180^\circ - \frac{\alpha}{2}$$

in which α is the cone apex angle and λ_c is used to indicate a smooth cone ($\lambda_c = 0$) or a rough cone ($\lambda_c = 1$).

Yu's analytical solution (28) has been extended recently by Su and Liao (2002) to include the effect of shear strength anisotropy (see Figure 11). The cone factor for soil obeying an anisotropic failure criterion is:

$$N_c = \frac{1 + A_r}{\sqrt{1 + 2A_r}} \ln I_r + \frac{1 - A_r}{3} + R \left\{ 1 + \frac{1 + A_r}{\sqrt{1 + 2A_r}} + 0.52 A_r^{1/8} (1 + A_r) \right\} \quad (29)$$

where $R = 3.13$ for a rough cone and $R = 1.39$ for a smooth cone. The shear strength anisotropy is defined by the parameter A_r , which is the ratio between the undrained shear strength from extension triaxial tests and that from compression tests.

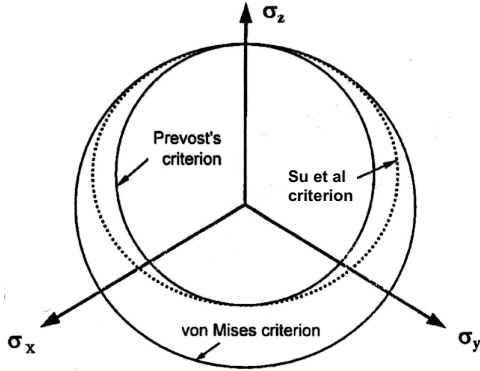


Figure 11: The anisotropic strength criteria (after Su and Liao, 2002)

A simple comparison between equations (28) and (29) indicates that the effect of strength anisotropy of clay will become significant only when the strength anisotropy ratio A_r is less than 0.6.

4.2.2 Strain path analysis combined with finite element methods

The analysis of cone penetration in a von Mises soil by combining strain path analysis and finite element calculations was used by Teh and Houlsby (1991) to overcome the inequilibrium problem of a pure strain path analysis. This combined analysis gives a slightly higher cone factor than that from a pure strain path analysis. The resulting cone factor is:

$$N_c = \left(1.67 + \frac{I_r}{1500} \right) (1 + \ln I_r) + 2.4\lambda_c - 0.2\lambda_s - 1.8\Delta \quad (30)$$

where λ_s and λ_c are used to indicate either rough (with a value of 1) or smooth interfaces (with a value of 0) for the shaft and cone respectively. The parameter $\Delta = (\sigma_{v0} - \sigma_{h0}) / (2S_u)$ is used to include the effect of anisotropic in situ stress states.

4.2.3 Steady state finite element analysis

Yu et al. (2000) developed a novel finite element formulation for the analysis of steady state cone penetration in undrained clay modelled by both the von Mises and modified Cam clay models. The proposed finite element analysis focuses on the total displacements experienced by soil particles at a particular instant in time during the cone penetration test. This is possible because, with the steady state assumption, the time dependence of stresses and

strains can be expressed as a space-dependence in the direction of penetration (see Figure 12). As a result, the finite element solution of steady cone penetration can be obtained in one step. This new analysis offers the following advantages over the strain path method:

- 1) All equations of soil equilibrium are fully accounted for.
- 2) Cone and shaft roughness can be taken into account in a more rigorous manner.
- 3) It can be more easily adapted to analyse cone penetration in dilatant soils.

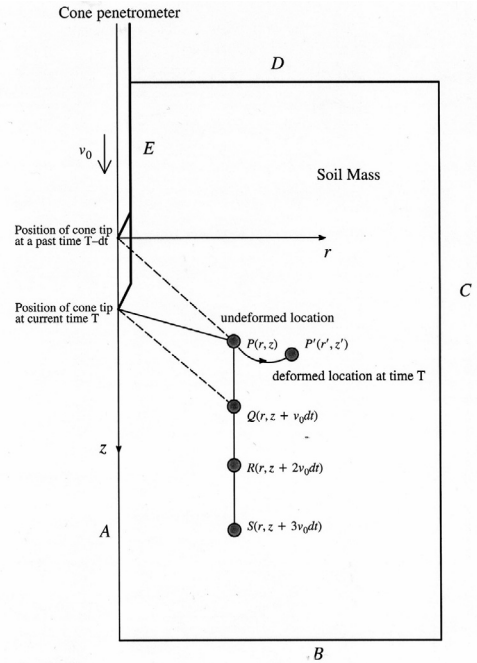


Figure 12: Steady state finite element analysis of cone penetration (after Yu et al., 2000)

The cone factor obtained by Yu et al. (2000) for a von Mises soil is given by the following equation:

$$N_c = 0.33 + 2 \ln I_r + 2.37\lambda - 1.83\Delta \quad (31)$$

where λ (ranging between 0 and 1) is used to indicate roughness of the cone/shaft and soil interface.

4.2.4 Cavity expansion combined with finite element analysis

Most recently, a numerical model has been presented by Abu-Farsakh et al. (2003) for the analysis of cone penetration in clay. As shown in Figure 13,

the penetration problem is numerically simulated in two stages. First, the cone penetrometer is expanded radially from a small initial radius to its radius and this is similar to a cylindrical cavity expansion process. Second, the continuous penetration of the penetrometer is simulated by imposing incremental vertical displacements on the nodes along the cone and soil interface. The cone factor from this combined cavity expansion and finite element analysis using the modified Cam clay model is given as follows:

$$N_c = 2.45 + 1.8 \ln I_r - 2.1 \Delta \quad (32)$$

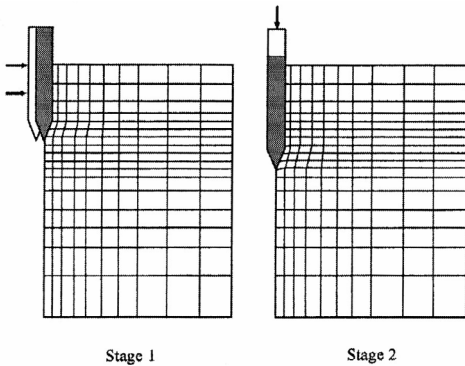


Figure 13: Combined cavity expansion and finite element analysis (after Abu-Farsakh et al., 2003)

4.2.5 Strain path analysis combined with cavity expansion methods

Yu and Whittle (1999) presented a novel approach to estimate the cone factor by making use of both strain path analysis and cavity expansion methods. With this new method, the strain path solution of a simple pile developed by Baligh (1986) for a von Mises soil was used to estimate the size of the plastic zone in the soil caused by cone penetration. Once the plastic region is established, spherical cavity expansion theory was then used to determine the stress distribution and therefore cone resistance. The cone factor for smooth cone and shaft derived from this hybrid method is:

$$N_c = 1.93 + 2 \ln I_r \quad (33)$$

which gives slightly higher values than those from a pure strain path analysis. For example, Baligh's strain path solution for a simple pile geometry is (van den Berg, 1994):

$$N_c = 1.51 + 2 \ln I_r \quad (34)$$

and the strain path solution of Teh and Houlsby (1991) for an actual cone geometry is:

$$N_c = 1.25 + 1.84 \ln I_r \quad (35)$$

4.2.6 Adaptive finite element analysis

Most recently, Lu (2004) presented a finite element analysis of cone penetration in clay using the adaptive remeshing technique proposed by Hu and Randolph (1998). The adaptive remeshing technique was first used for modelling metal forming processes (Cheng, 1988) and localisation problems (Lee and Bathe, 1994) to overcome the severe distortion in large deformation finite element analysis.

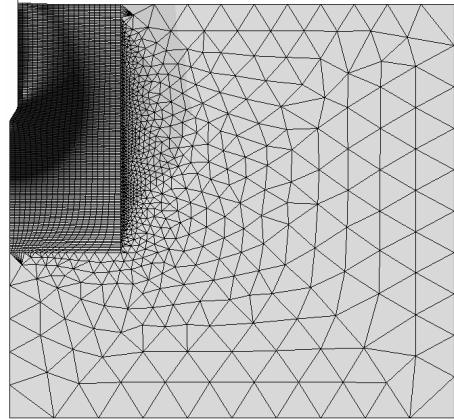


Figure 14: Deformed finite element mesh and plastic region due to cone penetration in clay

A similar finite element study was also carried out by the Author and his student Mr. J. Walker using the commercial finite element program, ABAQUS, with the option of adaptive meshing techniques. The adaptive meshing in ABAQUS is often referred to as Arbitrary Lagrangian-Eulerian (ALE) analysis. A deformed finite element mesh and the plastic region (represented by the dark area) generated by cone penetration in clay are shown in Figure 14. Soils were modelled by the von Mises criterion. In this approach, remeshing and remapping of the field variables from an old mesh to a new one are carried out at a prescribed frequency. A preliminary solution obtained for the cone factor for a smooth cone and shaft/soil interface can be written as follows:

$$N_c = 0.27 + 1.915 \ln I_r \quad (36)$$

The influence of in-situ stress states and the roughness of soil-shaft/cone interface can be readily accounted for using adaptive finite element analysis and is currently being studied at the University of Nottingham.

4.3 Consolidation coefficients

The coefficient of consolidation is one of the most difficult soil properties to measure in geotechnical engineering. As mentioned earlier, it can be measured in situ using self-boring pressuremeter holding tests to observe the excess pore pressure decay with time. The interpretation of the pressuremeter holding tests was based on the initial excess pore pressure derived from cavity expansion theory and one-dimensional consolidation solution.

A similar procedure has been used to measure the coefficient of consolidation using cone penetrometer with pore pressure measurement (i.e. CPTU or piezocone) by interrupting the cone penetration and observing the excess pore pressure decay with time. The interpretation of piezocone consolidation can be carried out by using either of the following two methods:

- One-dimensional cavity expansion methods (Torstenson, 1977; Randolph and Wroth, 1979).
- Two-dimensional strain path methods (Levadoux and Baligh, 1986; Baligh and Levadoux, 1986; Teh and Houlsby, 1991).

4.3.1 Cavity expansion approach

Torstenson (1977) developed an interpretation method based on cavity expansion theories. With this method, the initial excess pore pressures prior to consolidation were estimated using cavity expansion theories with an elastic-plastic soil model. It is noted in passing that more accurate solutions are now available with critical state models (Collins and Yu, 1996; Yu, 2000). The consolidation stage of the test was predicted using a one-dimensional, linear, uncoupled consolidation theory (i.e., neglecting the coupling between total stresses and pore pressures during consolidation).

As is the case in the pressuremeter holding tests, Torstenson (1977) suggested that the coefficient of consolidation should be interpreted at 50% dissipation from the following equation:

$$c = \frac{T_{50}}{t_{50}} r^2 \quad (37)$$

where T_{50} is a time factor which can be obtained from cavity expansion theory (Figure 3), r is the penetrometer radius, and t_{50} is the actual time taken for 50% consolidation (i.e. the excess pore pressure reduces to half of its initial value).

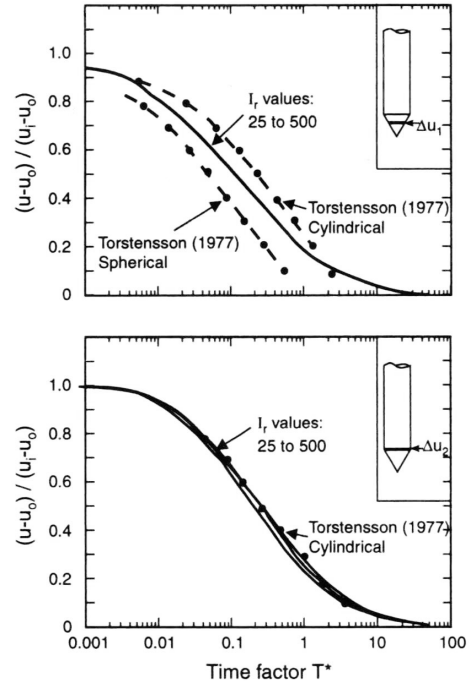


Figure 15: Theoretical solutions for consolidation around cones (after Teh and Houlsby, 1991 and Lunne et al., 1997)

It seems obvious that if the filter element for measuring pore pressures is located on the cone face the spherical cavity expansion solution would be more applicable. On the other hand, the cylindrical cavity expansion solution would be more suitable if the filter element is located on the shaft (Lunne et al., 1997).

4.3.2 Strain path approach

To account for the effect of the two-dimensional nature of cone penetration, Levadoux and Baligh (1986) and Baligh and Levadoux (1986) have used strain path methods (Baligh, 1985) to predict the excess pore pressures generated by the cone installation. Then a finite element method was used to carry out the subsequent coupled and uncoupled linear consolidation analysis. Their study led to some important conclusions including:

- 1) The effect of the coupling between total stresses and pore pressures is not very significant.
- 2) The initial distribution of the excess pore pressures has a significant influence on the dissipation process.
- 3) Dissipation is predominantly in the horizontal direction.

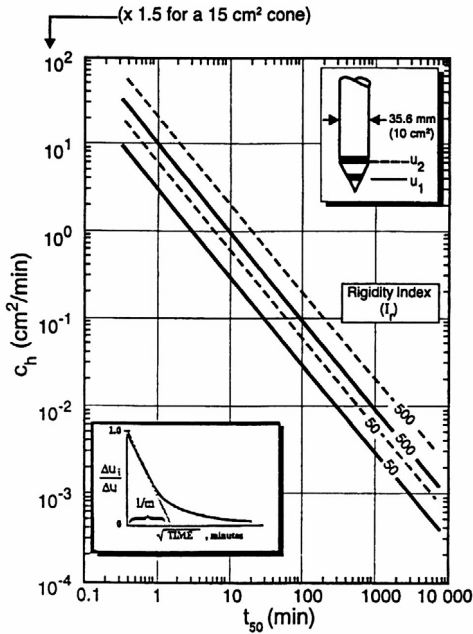


Figure 16: A chart for finding c_h from t_{50} (after Robertson et al., 1992)

By using a method similar to that of Baligh and Lavadoux (1986), Teh and Houlsby (1991) reported the results of a parametric study on cone penetration and consolidation. In the study of Teh and Houlsby, strain path analysis was used to determine the initial excess pore pressures and the subsequent uncoupled, linear consolidation was modelled by the finite difference method. To account for the effect of the stiffness index, $I_r = G/S_u$, Teh and Houlsby (1991) suggested the use of a modified dimensionless time factor, T^* , defined as

$$T^* = \frac{c_h t}{r^2 \sqrt{I_r}} \quad (38)$$

Figure 15 shows the strain path solutions of a normalised excess pore pressure versus the modified dimensionless time factor obtained by Teh and Houlsby (1991). For comparison, the cavity expansion solutions of Torstensson (1977) are also shown in the figure for two filter element locations with one immediately behind the cone and another on the cone face. It is most interesting to note that for the case with the filter element located immediately be-

hind the cone, the one-dimensional cavity expansion solutions are practically the same as the two-dimensional strain path solutions.

Based on the above theoretical solutions, Robertson et al. (1992) produced a chart (shown in Figure 16) that may be readily used to obtain the coefficient of consolidation from the actual time taken for 50% consolidation t_{50} .

4.4 Stress history - overconsolidation ratio

For clay, the overconsolidation ratio (OCR) is a key property that is needed to define its mechanical behaviour. Several approaches have been proposed to estimate the OCR from CPTU data (Lunne et al., 1997). In particular, Mayne (1993) proposed an analytical method based on cavity expansion theory and critical state soil mechanics. Mayne's method includes the following elements:

- 1) Use of Vesic's cavity expansion solution to estimate the cone factor (Vesic, 1977).
- 2) Use of critical state soil mechanics to link the undrained shear strength to the OCR (Wroth, 1984).
- 3) Use of spherical cavity expansion solutions and critical state soil mechanics to estimate excess pore pressures.

Based on the above assumptions, Mayne (1993) showed that the value of the OCR can be derived from CPTU data using

$$OCR = 2 \left\{ \frac{1}{1.95M + 1} \left(\frac{q_c - u_2}{\sigma'_{vo}} \right) \right\}^{1/\Lambda} \quad (39)$$

for the case with the filter element located behind the cone, and

$$OCR = 2 \left\{ \frac{1}{1.95M} \left(\frac{q_c - u_1}{\sigma'_{vo}} + 1 \right) \right\}^{1/\Lambda} \quad (40)$$

for the case with the filter element located on the cone face. In equations (39) and (40), u_1 and u_2 are pore pressures at the cone face and behind the cone respectively; M is the slope of the critical state line in the usual $q-p'$ plot; and Λ is a soil property typically in the range of 0.75-0.85 (Wroth, 1984).

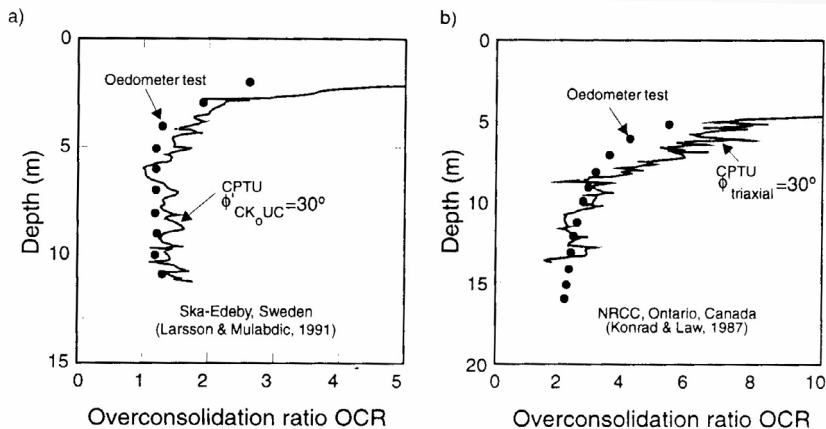


Figure 17: Measured and predicted *OCR* for sites in (a) Sweden and (b) Ontario (after Mayne, 1993)

Figure 17 demonstrated that the estimated values of the *OCR* using equation (39) from CPTU data are consistent with those measured using laboratory oedometer tests.

5 CONE PENETRATION TESTS IN SAND

5.1 Overview

Because of the dilatant characteristics of sand during shear, cone penetration in sand is much more difficult to analyse than that in undrained clay. Over the last two decades, good progress has been made in understanding the mechanics of cone penetration in undrained clay. By contrast, progress has been slow in developing rigorous methods to analyse cone penetration in cohesionless soil. This is why large laboratory chamber testing was widely used to develop empirical correlations between cone results and sand properties (e.g., Parkin and Lunne, 1982; Been et al., 1987; Houlsby and Hitchman, 1988; Ghionna and Jamiolkowski, 1991).

Most existing methods for the analysis of deep cone penetration in sand are based on either bearing capacity theory (Durgunoglu and Mitchell, 1975) or cavity expansion theory (Vesic, 1977; Yu and Mitchell, 1998; Salgado et al., 1997). In addition, attempts have also been made in using finite element and discrete element methods to simulate deep penetration problems in sand (van den Berg, 1994; Huang et al., 2004; Huang and Ma, 1994; Yu et al., 2004).

Cone penetration testing in sand is generally drained and therefore the analysis methods presented here are based on the assumption that there would be

no excess pore pressures generated as a result of cone penetration.

5.2 Drained shear strength

Cone tip resistance in sand is often used to derive soil friction angle. Various correlations have been proposed in this aspect and most of them were based on either bearing capacity analysis or cavity expansion theory.

5.2.1 Bearing capacity approach

Durgunoglu and Mitchell (1975) presented a well-known bearing capacity solution for deep cone penetration problems. A major advantage of this approach is its relative simplicity. This approach can be easily accepted by the engineer who is already familiar with bearing capacity calculations. As pointed out by Yu and Mitchell (1998), however, the major limitation of bearing capacity theory for cone penetration modelling in sand is its inability of accounting for soil stiffness and volume change.

In the study of Durgunoglu and Mitchell (1975), a failure mechanism was used to give a plane strain solution first (i.e. for wedge penetration). Then an empirical shape factor was used to account for the axisymmetric geometry of cone penetration problems. For the case when the soil-cone interface friction angle is half of the soil friction angle, the solution of Durgunoglu and Mitchell (1975) may be expressed by a simple expression:

$$N_q = \frac{q'_c}{\sigma'_{v0}} = 0.194 \exp(7.63 \tan \phi) \quad (41)$$

where N_q is the cone factor in sand and ϕ is drained soil friction angle.

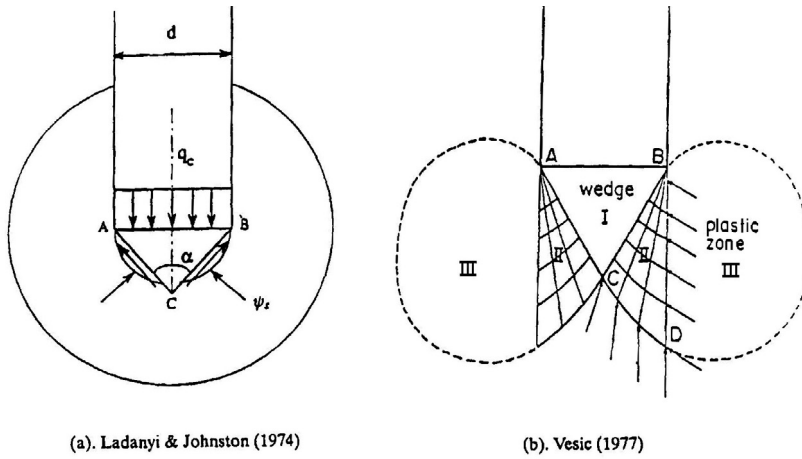


Figure 18: Mechanisms linking cone resistance with cavity limit pressures (after Yu and Mitchell, 1998)

5.2.2 Cavity expansion approach

The analogy between cavity expansion and cone penetration was first pointed out by Bishop et al. (1945) after observing that the pressure required to produce a deep hole in an elastic-plastic medium is proportional to that necessary to expand a cavity of the same volume under the same conditions. As discussed by Yu and Mitchell (1996, 1998), proposals were made by many researchers to relate cone tip resistance with cavity (mainly spherical cavities) limit pressures, which include those by Ladanyi and Johnston (1974) and Vesic (1977) - see Figure 18.

For example, Vesic (1977) assumed that cone tip resistance is related to the spherical cavity limit pressure by a failure mechanism shown in Figure 18(b). This assumption leads to the following simple expression of the cone factor:

$$N_q = \left(\frac{1+2K_0}{3-\sin\phi} \right) \exp \left[\left(\frac{\pi}{2} - \phi \right) \tan\phi \right] \times \tan^2 \left(\frac{\pi}{4} + \frac{\phi}{2} \right) (I_{rr})^n \quad (42)$$

in which $K_0 = \sigma'_{h0} / \sigma'_{v0}$, and $I_{rr} = I_s / (1 + I_s \varepsilon_v)$ is the reduced rigidity index where ε_v is the average volumetric strain estimated in the plastically deforming region, and the rigidity index I_s and parameter n are given by $I_s = G / (p'_0 \tan\phi)$ and $n = 4 \sin\phi / [3(1 + \sin\phi)]$.

After applying the Vesic correlation to the results of a number of chamber tests, Mitchell and Keaveny (1986) concluded that measured cone resistances

may be closely modelled for sands with a low value of the reduced index (i.e. more compressible soils). Since dilation was not accounted for in Vesic's solution, this approach cannot be used to model cone penetration in medium dense to very dense sands where dilation is significant.

To extend Vesic's approach, Salgado (1993) and Salgado et al (1997) used a stress rotation analysis to relate cone resistance to a cylindrical cavity limit pressure (see Figure 19). Based on a number of simplifying assumptions, cone resistance is linked to the cylindrical cavity limit pressure as follows:

$$q'_c = 2 \exp(\pi \tan\phi) \frac{[(1+C)^{1+l} - (1+l)C - 1]}{C^2 l (1+l)} P'_{lc} \quad (43)$$

where P'_{lc} denotes the effective cylindrical cavity limit pressure, l is determined numerically and C is linked to soil dilation angle ψ by

$$C = \sqrt{3} \exp \left(\frac{\pi}{2} \tan\psi \right).$$

Salgado et al. (1997) applied the theoretical correlation (43) to predict measured cone resistances for a large number of cone tests in large calibration chambers and concluded that the correlation worked well. Typically the measured cone resistances can be predicted to within 30%.

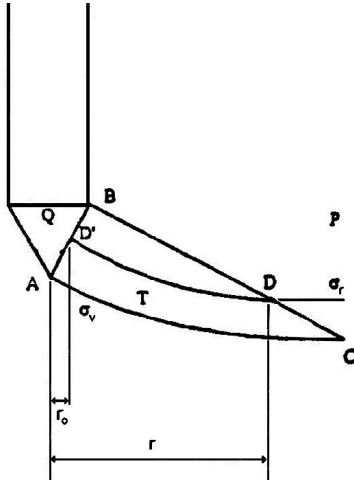


Figure 19: Linking cone resistance with cylindrical cavity limit pressure (after Salgado, 1993)

By using both numerical cavity expansion solutions and chamber data for cone tip resistance, Cudmani and Osinov (2001) recently proposed the following average equation to link cone tip resistance q'_c with the spherical cavity limit pressure P'_{ls} :

$$q'_c = \left[1.5 + \frac{5.8(D_r)^2}{(D_r)^2 + 0.11} \right] P'_{ls} \quad (44)$$

where D_r is the relative density ranging between 0 and 1. Note that in the study of Cudmani and Osinov, a slightly different, pressure-dependent relative density was considered. Cudmani and Osinov (2001) showed that equation (44) is able to predict 85% of their chamber test data of cone tip resistances to within 25%.

5.2.3 Combined cylindrical-spherical cavity expansion method

All the cavity expansion methods described in the previous section assumed that cone tip resistance is related, through theoretical or semi-analytical considerations, to either spherical cavity limit pressure or cylindrical cavity limit pressure. Here a new method is proposed to estimate cone tip resistance by using both cylindrical and spherical cavity expansion solutions. The basic idea of the new method consists of two steps:

- 1) Estimate of the size of the plastically deforming zone around the cone using the cylindrical cavity solution for the size of the plastic region.

- 2) Use of spherical cavity expansion theory to determine the cone tip resistance from the estimated plastic region.

This approach was motivated by a recent finite element study of cone penetration in sand (Huang et al., 2004), which suggests that the plastic zone behind the cone and around the shaft is similar to that predicted by the cylindrical cavity expansion theory. Around the cone tip and face, the elastic-plastic boundary may be assumed to be circular or elliptical in shape (see Figure 20).

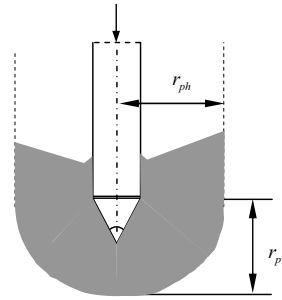


Figure 20: Plastic zone around a cone in sand (after Huang et al., 2004)

By following the above procedure and using the cavity expansion solutions in Mohr-Coulomb materials, as derived by Yu (2000) and Yu and Carter (2002), cone tip resistance for a purely frictional soil is given by:

$$\frac{q'_c}{p'_0} = \frac{3\alpha'}{2 + \alpha'} \left(F \frac{c}{a} \right)^{\frac{2(\alpha'-1)}{\alpha'}} \quad (45)$$

where F is a plastic zone shape factor that takes a value of unity if the plastic zone around the cone is a circle (i.e. $r_{ph} = r_{pv}$) and otherwise would be less than 1. Pending more numerical studies, F may be assumed to be between 0.7-0.8 and (c/a) denotes the relative size of the plastic zone generated by the expansion of a cylindrical cavity from zero radius. Yu (2000) derived an analytical solution for this quantity, which can be readily obtained by solving the following simple non-linear equation for a purely frictional soil:

$$1 = \gamma \left(\frac{c}{a} \right)^{\frac{\alpha'-1}{\alpha'}} + [2\delta - \gamma] \left(\frac{c}{a} \right)^{\frac{\beta'+1}{\beta'}}$$

in which

$$\gamma = \frac{\alpha' \beta' s'}{\alpha' + \beta'}, \quad \delta = \frac{(\alpha' - 1)p'_0}{2(1 + \alpha')G}, \quad s' = \frac{\chi(1 - \alpha')}{\alpha' \beta'}$$

$$\alpha' = \frac{1 + \sin \phi}{1 - \sin \phi}, \quad \beta' = \frac{1 + \sin \psi}{1 - \sin \psi},$$

$$\chi = \frac{(1 - \nu)\alpha' p'_0}{((\alpha')^2 - 1)G} \left\{ \left[\beta' - \frac{\nu}{1 - \nu} \right] + \frac{1}{\alpha'} \left[1 - \frac{\nu \beta'}{1 - \nu} \right] \right\}$$

and ν is Poisson's ratio. It is noted that following the same procedure, the solution for the cone tip resistance in a cohesive-frictional soil can also be obtained in closed form using the cavity expansion solutions derived by Yu (2000).

5.3 In situ state parameter

Based on the results of a large number of cone tests in calibration chambers, Been et al. (1987) were the first to observe that cone tip resistance may correlate with the initial (in situ or pre-shear) state parameter. Their empirical correlation between the cone resistance and the initial state parameter is given in the following form:

$$\frac{q'_c}{p'_0} = k \exp(-m \xi_0) + 1 \quad (46)$$

After a more detailed analysis of chamber test data on Ticino sand, Sladen (1989) later showed that this correlation is not unique, rather the relationship varies significantly with mean stress level. In other words, the coefficients k and m in equation (46) are not constants even for the same sand.

Yu and Mitchell (1996, 1998) provided a theoretical explanation for such a pressure-dependent, cone resistance-state parameter relationship. Using a state parameter soil model, Collins et al. (1992) found that the spherical cavity limit pressure is linked to the initial mean stress and void ratio as follows:

$$\frac{P'_{ls}}{p'_0} = m_1 (p'_0)^{(m_2 + m_3 v_0)} \exp(-m_4 v_0) \quad (47)$$

where $v_0 = 1 + e_0$ is the initial specific volume of the soil and e_0 is the initial void ratio. For Ticino sand, the constants are: $m_1 = 2.012 \times 10^7$, $m_2 = -0.875$, $m_3 = 0.326$, $m_4 = 6.481$.

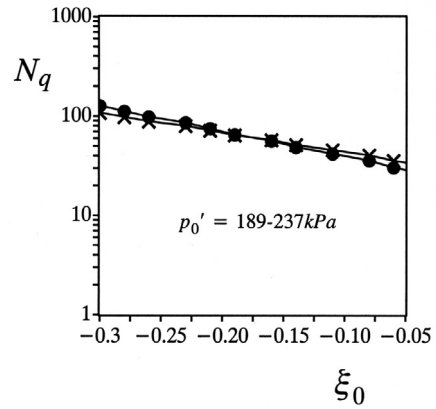
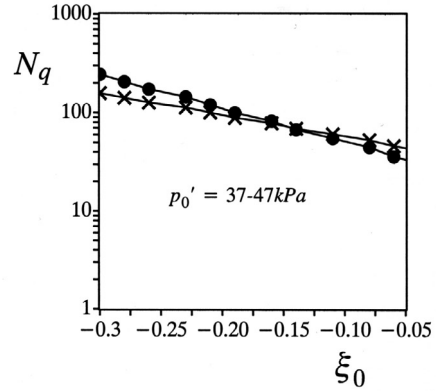


Figure 21: Measured (cross) and predicted (solid circle) cone factor-state parameter relations (after Yu and Mitchell, 1998)

Yu and Mitchell (1998) then used the correlation of Ladanyi and Johnston (1974) to estimate cone tip resistance from the spherical cavity limit pressure determined from equation (47). Presented in Figure 21 are comparisons between cavity expansion predictions and experimental data for chamber cone test results in Ticino sand at two different stress levels. The experimental curves were obtained by applying a chamber size correction factor (given by Been et al., 1987) to the best-fit lines presented by Sladen (1989). It is clear from the figure that a good agreement was obtained.

Russell and Khalili (2002) recently extended the cavity expansion solution of Collins et al. (1992) and showed that the theoretical correlation between spherical cavity limit pressure and initial state parameter is also strongly affected by particle crushing which was reflected by a steeper critical state line at high stress level. Particle crushing was also shown experimentally by Konrad (1998) as an important

factor in the interpretation of state parameters from cone penetration tests in a calibration chamber.

6 CONE PRESSUREMETER TESTS IN CLAY AND SAND

6.1 Overview

The cone pressuremeter (also known as the full-displacement pressuremeter) is an in situ testing device that combines a standard cone penetrometer with a pressuremeter module incorporated behind the cone tip. The idea of mounting a pressuremeter module behind the cone tip was first introduced in the early 1980s. The development aims to combine the merits of both the standard cone and the pressuremeter into a single instrument. The cone pressuremeter can be installed by standard CPT jacking equipment and this enables pressuremeter tests to be carried out as part of routine CPT operations (see Figure 22).

Cone pressuremeter tests are difficult to analyse because the tests are carried out in a soil that has already been disturbed by the penetration of the cone (Withers et al., 1989). As a result, a rigorous interpretation of cone pressuremeter tests must account for the effect of installation process. This is why the development of equipment for the cone pressuremeter was, for a long time, more advanced than its interpretation methods. So far, the analytical interpretation methods for cone pressuremeter tests have been mainly based on cavity expansion/contraction theory (Houlsby and Withers, 1988; Yu et al., 1996).

6.2 Cone pressuremeter tests in undrained clay

Using cavity expansion theory, Houlsby and Withers (1988) developed the first theoretical interpretation method for deriving soil properties from cone pressuremeter tests in undrained clay. In the analysis, the initial installation of the instrument was modelled as the expansion of a cylindrical cavity in the soil. The expansion phase of cone pressuremeter tests was modelled as a continuous expansion of the same cavity, and the unloading phase of the tests as the cavity contraction.

This one-dimensional simulation of cone penetration is somewhat in error because it ignores the two-dimensional nature of the problem. However more rigorous, two-dimensional analyses of the cone penetration problem (e.g., Baligh, 1986; Teh and Houlsby, 1991; Yu et al., 2000) show that the stress distribution far behind the cone is similar to that obtained from the expansion of a cylindrical cavity from zero radius. Given the pressuremeter module is

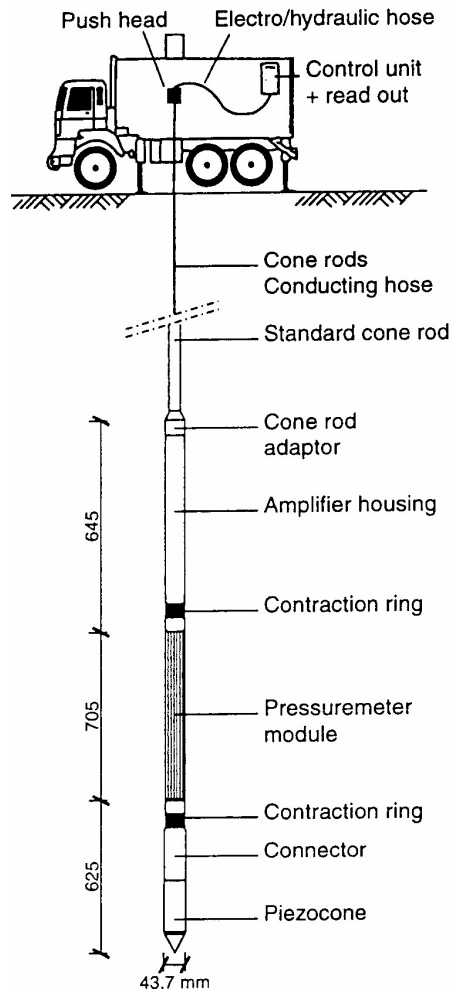


Figure 22: A cone pressuremeter (after Withers et al., 1989)

located some distance from the cone, it seems sensible to use a simple cavity expansion theory as the basis for the interpretation of cone pressuremeter test results.

Since the installation and subsequent expansion of the cone pressuremeter is simulated as the expansion of a cylindrical cavity from zero radius, it can be easily shown that the cavity pressure remains constant during any stage of installation and loading tests. The constant pressure is the same as the limiting pressure obtained from the expansion of a cavity from a finite radius (Yu and Houlsby, 1991). For a Tresca soil, the limiting pressure is well known (Gibson and Anderson, 1961):

$$P_{\max} = \sigma_{h0} + S_u (1 + \ln I_r) \quad (48)$$

The complete analytical solution for pressuremeter unloading curves is defined by the following equation:

$$P = P_{\max} - 2S_u \{1 + \ln[(\varepsilon_c)_{\max} - \varepsilon_c] + \ln I_r\} \quad (49)$$

where $(\varepsilon_c)_{\max}$ is the maximum cavity strain at the start of cone pressuremeter unloading tests. The above solution is plotted in Figure 23, which shows that the slope of the unloading plastic curve in a plot of P versus $-\ln[(\varepsilon_c)_{\max} - \varepsilon_c]$ is equal to $2S_u$. From the figure, both shear modulus and initial horizontal total stress may also be estimated.

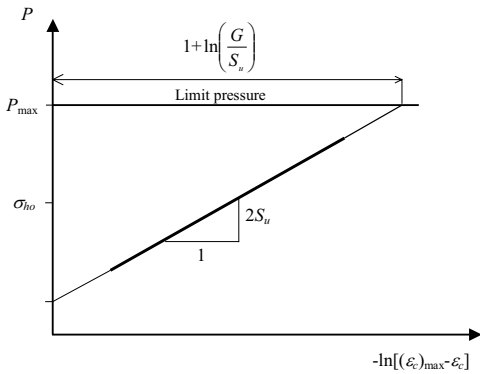


Figure 23: The interpretation method of Houlsby and Withers (1988)

6.3 Cone pressuremeter tests in sand

For obvious reasons, rigorous analysis of cone pressuremeter tests in sand is extremely difficult. Using a non-associated Mohr-Coulomb model, Yu (1990) derived a large strain cavity expansion/contraction solution for sand, equivalent to that of Houlsby and Withers (1988) for clay (see also Yu and Houlsby, 1991 and 1995). However, limited applications of this solution in the interpretation of cone pressuremeter tests in sand suggested that it could give unrealistic soil properties. This indicates that soil behaviour during cone pressuremeter tests may be too complex to be modelled accurately by a perfectly plastic Mohr-Coulomb model.

Using both cone tip resistance and pressuremeter limit pressure measured with a cone pressuremeter, Yu et al. (1996) proposed a semi-analytical method for deriving the soil friction angle and the in situ state parameter. In this approach, it was assumed that pressuremeter limit pressure can be estimated by the limit pressure from cylindrical cavity expansion.

The cone tip resistance was estimated from the limit pressure of spherical cavity expansion using the correlation of Ladanyi and Johnston (1974). Therefore the theoretical ratio of cone resistance and pressuremeter limit pressure (ψ'_i) can be expressed in terms of the ratio of spherical cavity limit pressure to cylindrical cavity limit pressure as follows:

$$\frac{q'_c}{\psi'_i} = (1 + \sqrt{3} \tan \phi) \frac{P'_{ls}}{P'_{lc}} \quad (50)$$

For the determination of the friction angle, cavity expansion solutions in a perfectly plastic Mohr-Coulomb soil were used. In the evaluation of the in situ state parameter, cavity expansion solutions using a state parameter-based, critical state model were used (Collins et al., 1992; Yu, 2000).

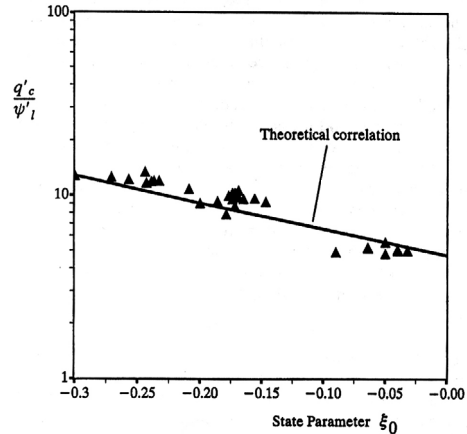


Figure 24: Measured and theoretical correlations for cone pressuremeter tests in Leighton Buzzard sand (after Yu et al., 1996)

6.3.1 Drained shear strength

Yu et al. (1996) used the analytical cavity limit pressures of Yu and Houlsby (1991) to correlate the ratio of cone tip resistance to pressuremeter limit pressure with the angle of soil friction. After a parametric study, Yu et al. (1996) proposed the following correlation:

$$\phi = 22.7 + \frac{14.7}{\ln(G/p'_0)} \times \frac{q'_c}{\psi'_i} \quad (51)$$

which may be used to derive friction angles from measured ratio of q'_c/ψ'_i , provided a reasonable estimate can be made for stiffness index G/p'_0 .

6.3.2 *In situ state parameter*

Using a state parameter-based, critical state soil model, Collins et al. (1992) presented the limit pressure solutions for the expansion of both spherical and cylindrical cavities in six different sands that have been widely used for calibration chamber testing. The results of these numerical solutions suggest that the ratio of spherical and cylindrical cavity limit pressures may be estimated by the following equation:

$$\frac{P'_{ls}}{P'_{lc}} = C_1 (p'_0)^{C_2 + C_3(1+e_0)} \exp[C_4(1+e_0)] \quad (52)$$

where e_0 is the initial void ratio and the constants C_1, C_2, C_3, C_4 for the six reference sands are given in Table 2.

Table 2. Material constants (Collins et al., 1992)

| Sand | C_1 | C_2 | C_3 | C_4 |
|----------------|-------|--------|-------|--------|
| Monterrey No 0 | 1087 | -0.47 | 0.225 | -3.214 |
| Hokksund | 560 | -0.424 | 0.195 | -2.84 |
| Kogyuk | 237 | -0.359 | 0.167 | -2.485 |
| Ottawa | 1163 | -0.469 | 0.24 | -3.483 |
| Reid Bedford | 342 | -0.385 | 0.172 | -2.521 |
| Ticino | 376 | -0.387 | 0.175 | -2.604 |

Yu et al. (1996) showed that the theoretical correlation between the ratio q'_c/ψ'_i and the in situ state parameter ξ_0 is largely independent of initial stress level. In addition its dependence on sand type was also found to be small. The following average correlation was therefore proposed by Yu et al. (1996) for practical applications:

$$\xi_0 = 0.4575 - 0.2966 \ln \frac{q'_c}{\psi'_i} \quad (53)$$

This can be used to derive the in situ state parameter from the measured ratio of q'_c/ψ'_i .

The theoretical correlation (53) was supported by experimental results presented in Yu et al. (1996) for cone pressuremeter tests in sand (see Figure 24). Its relevance has also been demonstrated by Robertson et al. (2000) using both cone and self-boring pressuremeter test data from the Canadian Liquefaction Experiment (CANLEX) project. Powell and Shields (1997) applied this theoretical correlation to obtain in situ state parameters from field cone pressuremeter tests in sand.

6.4 *Effect of finite pressuremeter length*

Like self-boring pressuremeters, cone pressuremeters have a finite length to diameter ratio (typically around 10) and therefore the one-dimensional analysis of Houlsby and Withers (1988) may lead to errors in the derived soil properties. To quantify these errors, Yu (1990) carried out a large strain finite element analysis of cone pressuremeter tests. In this analysis, the installation of the cone pressuremeter was modelled as the expansion of a cylindrical cavity. The stress field at the end of the installation can be obtained from analytical cavity expansion solutions. Then starting from this initial stress state, a large strain finite element formulation was used to analyse the expansion and contraction of the pressuremeter membrane. The parametric study reported by Yu (1990, 1993a) for a pressuremeter length to diameter ratio of 10 leads to the following conclusions:

- 1) The one-dimensional analysis of Houlsby and Withers (1988) overestimates the undrained shear strength and this overestimate could be as high as 10% for a high stiffness index.
- 2) The neglect of finite pressuremeter length underestimates the shear modulus and this underestimate may increase to 20% for a high stiffness index.
- 3) The one-dimensional analysis leads to very significant errors in the derived in situ total horizontal stress. The corrected in situ total horizontal stress after accounting for finite pressuremeter length is:

$$(\sigma_{h0})^c = \sigma_{h0} - 0.63S_u - 0.073S_u \ln I_r \quad (54)$$

where σ_{h0} is the in situ total horizontal stress derived directly from the one-dimensional analysis of Houlsby and Withers (1988).

Yu (1990) applied equation (54) to the cone pressuremeter test data reported by Houlsby and Withers (1988) and found that the measured total horizontal stresses with finite length corrections are consistent with those measured from self-boring pressuremeter tests (see Figure 25). This has been further confirmed recently by Powell (2004) after applying equation (54) to a large number of cone pressuremeter tests in other clays.

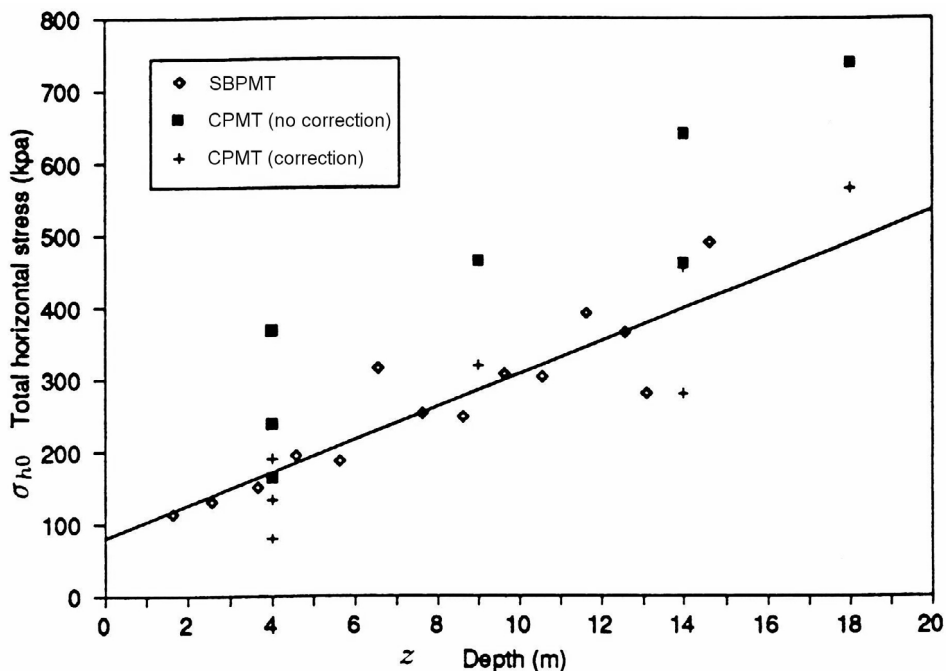


Figure 25: Measured in situ horizontal stresses with various methods for tests at Madingley, Cambridge (after Yu, 1990)

7 FLAT DILATOMETER TESTS IN CLAY

7.1 Overview

The flat dilatometer (shown in Figure 26) is being used increasingly in geotechnical practice to obtain design parameters for a variety of soils (Marchetti, 1980; Marchetti et al., 2001). This is because

- 1) It is simple to operate and maintain.
- 2) It does not rely on minimizing disturbance during insertion.
- 3) It provides a repeatable and continuous profile of the measured parameters.

To date, however, the interpretation of the test has been performed almost exclusively using empirical methods (Marchetti, 1980; Lutenegeger, 1988; Campanella and Robertson, 1991; Mayne and Martin, 1998). Research aiming at a better understanding of the fundamental mechanics of the dilatometer test is very limited and seems to be only related to tests in undrained clay. These existing studies were based on either strain path analysis (Huang, 1989; Finno,

1993; Whittle and Aubeny, 1993) or flat cavity expansion methods (Yu et al., 1993; Smith and Houlsby, 1995).

7.2 Total stress flat cavity expansion analysis

As a simple model, Yu et al. (1993) proposed that the installation of a flat dilatometer can be simulated as a flat cavity expansion process. This is consistent with the usual practice of modelling cone pressuremeter installation as a cylindrical cavity expansion process (Houlsby and Withers, 1988). The difference is that no analytical solutions are available for the expansion of a flat cavity in soils. Therefore numerical methods must be used for modelling dilatometer tests. Whilst it is expected that the simple two-dimensional flat cavity expansion modelling approach will introduce errors in the calculated stresses close to the tip of the dilatometer blade, the stresses predicted at some distance behind the dilatometer tip would be reasonably accurate (Finno, 1993).

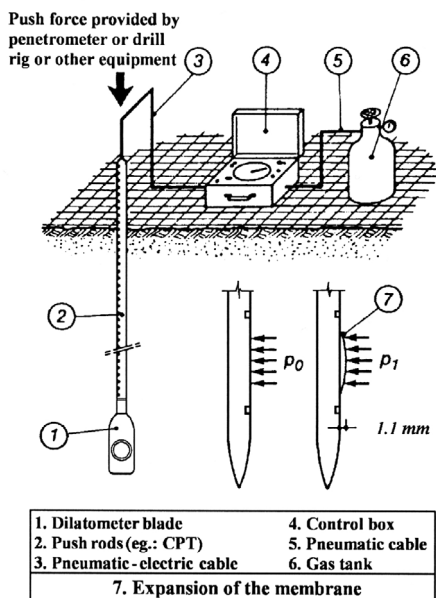


Figure 26: Setup and procedure of the flat dilatometer testing (after Marchetti et al., 2001)

By using a linear elastic-perfectly plastic Tresca soil model, Yu et al. (1993) conducted a finite element analysis of the dilatometer installation. The numerical results showed that the first pressure reading (i.e. lift-off pressure) of the dilatometer P_0 can be linked to the in situ total horizontal stress σ_{h0} and stiffness index $I_r = G/S_u$ in terms of a dilatometer factor N_{p_0} as follows:

$$N_{p_0} = \frac{P_0 - \sigma_{h0}}{S_u} = 1.57 \ln I_r - 1.75 \quad (55)$$

The numerical study indicates that the lift-off pressure of the dilatometer is similar to that of a cone pressurometer. This theoretical finding is in agreement with experimental observation (Lutenegger and Blanchard, 1990).

In addition, Yu et al. (1993) noted that the dilatometer factor N_{p_0} may be usefully linked to the dilatometer horizontal stress index K_D and the coefficient of earth pressure at rest $K_0 = \sigma'_{h0}/\sigma'_{v0}$ as follows:

$$K_D - K_0 = N_{p_0} \times \frac{S_u}{\sigma'_{v0}} \quad (56)$$

7.3 Effective stress flat cavity expansion analysis

To account for the effect of soil stress history, the installation of the dilatometer into undrained clay can be analysed using an effective stress formulation in conjunction with a critical state model. Together with his student Mr. C. Khong, the Author has carried out a parametric study using the critical state model CASM which was developed by Yu (1998). The model CASM has been implemented into the finite element programme CRISP, which was then used in dilatometer analyses. The material constants used are relevant to three different clays as given in Table 3.

Table 3: Clay constants used in CASM

| Clay | London clay | Weald clay | Speswhite kaolin clay |
|-----------|-------------|------------|-----------------------|
| M | 0.89 | 0.9 | 0.86 |
| λ | 0.161 | 0.093 | 0.19 |
| κ | 0.062 | 0.025 | 0.03 |
| μ | 0.3 | 0.3 | 0.3 |
| Γ | 2.759 | 2.06 | 3.056 |
| n | 2.0 | 4.5 | 2.0 |
| r | 2.718 | 2.718 | 2.718 |

For a given clay, it is possible numerically to relate the dilatometer factor, N_{p_0} , with the overconsolidation ratio of the soil. It is well known that OCR is used to denote the overconsolidation ratio defined in terms of vertical effective stress. Overconsolidation ratios can also be defined in terms of mean effective stress, which is usually denoted by R (Wroth, 1984). The exact relationship between these two overconsolidation ratios is complex and depends on the actual consolidation history of the soil. For example, they become identical for an isotropically consolidated soil sample (Wroth, 1984) and for a one-dimensionally consolidated sample it may be shown that R tends to be somewhat smaller than OCR (Wood, 1990).

The preliminary numerical studies reported here refer to the plane strain analysis of a dilatometer installation into an isotropically consolidated clay, and in this case the two definitions of overconsolidation ratio become identical. As shown in Figure 27, the finite element results indicate that the dilatometer factor may be linked to the initial state (overconsolidation ratio) of the clay by the following form:

$$N_{p_0} = \frac{P_0 - \sigma_{h0}}{S_u} = c_1 (OCR)^{c_2} \quad (57)$$

where c_1 and c_2 are constants depending on material type. For the three clays used, their values are: $c_1 = 6.17$ and $c_2 = -0.086$ for London clay; $c_1 = 7.24$ and $c_2 = -0.121$ for Weald clay; and $c_1 = 6.65$ and $c_2 = -0.046$ for Kaolin clay.

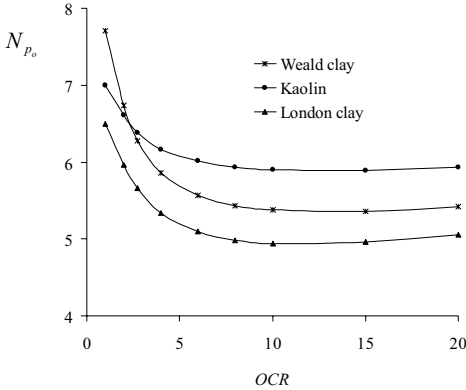


Figure 27: Theoretical correlation between dilatometer index and OCR

By combining equations (57) and (56), we can obtain the following relationship:

$$K_D - K_0 = c_1 (OCR)^{c_2} \times \frac{S_u}{\sigma'_{v0}} \quad (58)$$

Wroth (1984) showed that for isotropically consolidated soils the critical state theory links the undrained strength ratio to the OCR in an elegant form:

$$\frac{S_u}{\sigma'_{v0}} = \frac{M}{2} \left(\frac{OCR}{r} \right)^\Lambda \quad (59)$$

where r is the spacing ratio (Yu, 1998) and $\Lambda = (\lambda - \kappa)/\lambda$. The validity of this theoretical prediction has been confirmed by experimental data (Ladd et al., 1977). In addition, Mayne and Kulhawy (1982) showed that K_0 may be empirically related to the OCR as follows:

$$K_0 = (1 - \sin \phi)(OCR)^{\sin \phi} \quad (60)$$

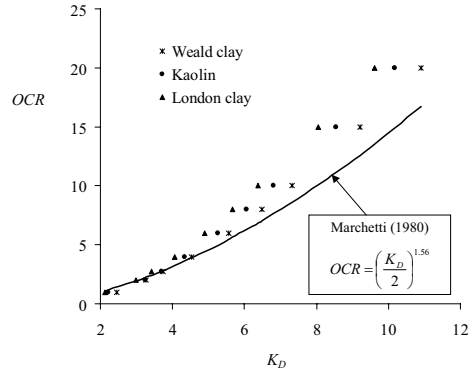


Figure 28: Theoretical correlation between K_D and OCR

By using equations (59) and (60) and noting $\sin \phi = 3M/(6 + M)$, equation (56) gives a theoretical correlation between K_D and the OCR:

$$K_D = \frac{6 - 2M}{6 + M} (OCR)^{\frac{3M}{6+M}} + \frac{c_1 M}{2r^\Lambda} (OCR)^{c_2 + \Lambda} \quad (61)$$

which is shown in Figure 28 for the three clays considered.

Furthermore, equations (60) and (61) can be combined to give the following correlation between K_D and K_0 :

$$K_D = K_0 + \frac{c_1 M}{2r^\Lambda} \left[\frac{(6 + M)}{(6 - 2M)} K_0 \right]^{\frac{6+M}{3M}(c_2 + \Lambda)} \quad (62)$$

which is shown in Figure 29 for the three clays considered.

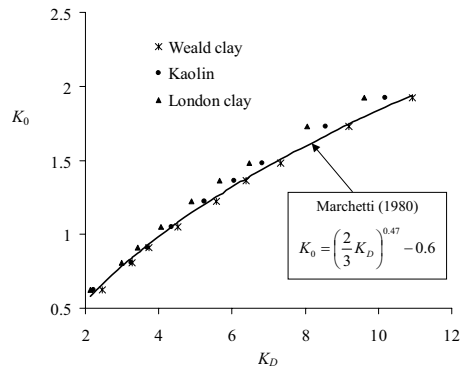


Figure 29: Theoretical correlation between K_D and K_0

It is clear from these comparisons that whilst the empirical correlations of Marchetti (1980) may be reasonable for some clays, they could be very inaccurate for others depending on their mechanical properties. In particular, the theoretical $OCR - K_D$ correlations for the three clays considered show considerable differences from the Marchetti correlation. This difference was also observed by Powell and Uglow (1988) when comparing the Marchetti's correlations with field dilatometer test data obtained in several UK clays.

7.4 Strain path analysis

In an important contribution, Huang (1989) implemented a numerical technique to conduct strain path analysis for arbitrary three-dimensional penetrometers. Further strain path analyses of the installation of flat dilatometers in clays were reported by Whittle and Aubeny (1993) and Finno (1993).

Whilst these studies have provided useful insights, their scopes were rather limited and no theoretical correlations were produced for direct use in practice. The parametric study reported by Finno (1993), using a bounding surface soil model for relatively low OCR values, seems to support the empirical correlation between K_D and the OCR proposed by Marchetti (1980).

8 FLAT DILATOMETER TESTS IN SAND

8.1 Overview

Very little work has been published on the analysis of dilatometer tests in sand. The existing correlations are almost entirely empirical in nature. Due to volume changes, it is not straightforward to extend strain path analysis to sand. However, the approach of simulating dilatometer installation as a flat cavity expansion process can be equally used for both clay and sand.

Presented below are the results of finite element simulations of the installation of a dilatometer in sand performed by the Author and his students Mr. C.D. Khong and Mr. X. Yuan.

8.2 Drained shear strength

Following the study of Yu et al. (1993) in clay, the insertion of a dilatometer in sand has been modelled as a flat cavity expansion process. First we model the sand using a linear elastic, perfectly/plastic Mohr-Coulomb theory. The aim of the study is to theoretically link the dilatometer horizontal index K_D with the fundamental soil properties. The commercial finite element package, ABAQUS, was used

in the numerical simulations with the Mohr-Coulomb model.

In the parametric study reported here, the friction angle ϕ varies from 30 to 50 degrees. In addition, soil stiffness index (G/p'_0) is varied from 200 to 1500. The dilation angle ψ is derived from the angle of friction using Rowe's stress dilatancy relation (Bolton, 1986) by assuming a value of 30° for the critical state friction angle.

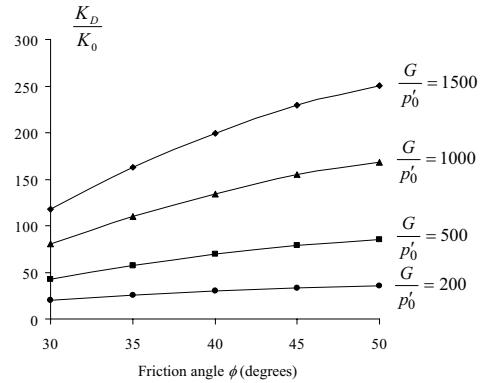


Figure 30: Theoretical correlation for deriving friction angle

Figure 30 shows that whilst the normalised dilatometer horizontal index K_D/K_0 increases with soil friction angle, the influence of the soil stiffness index G/p'_0 is also very significant. This is because a large initial part of the dilatometer insertion process occurs when soil is in an elastic state. As a result, the first reading of the dilatometer is a strong function of soil stiffness.

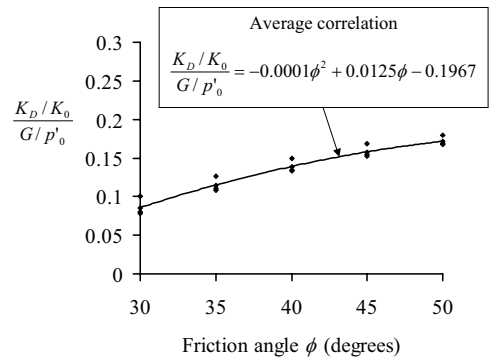


Figure 31: Normalised correlation for deriving friction angle

The numerical results presented in Figure 30 are re-presented in Figure 31 so that a single equation

may be used to relate the normalised horizontal index with friction angle and stiffness index, namely

$$\phi = 1013 \left[\frac{K_D/K_0}{G/p'_0} \right]^2 - 42.4 \left[\frac{K_D/K_0}{G/p'_0} \right] + 26.5 \quad (63)$$

which clearly shows that estimates for both the stiffness index and the in-situ horizontal stress coefficient must be made before the angle of soil friction can be deduced from K_D values measured from the dilatometer tests.

8.3 In situ state parameter

As a better alternative to the perfectly plastic Mohr-Coulomb theory, the unified state parameter model CASM (Yu, 1998) can be used to model sand behaviour. A previous section reported that CASM has been used successfully to model dilatometer tests in undrained clay. Here we report the results of a finite element analysis of the dilatometer installation in sand modelled by CASM. Like most other critical state models, CASM uses a pressure-dependent shear modulus. The parametric study reported here uses material model constants relevant to four well-known reference sands, listed in Table 4.

Table 4. Sand constants used in CASM

| Sand | Hokksund sand | Kogyuk sand | Ticino sand | Reid Bedford sand |
|-----------|---------------|-------------|-------------|-------------------|
| M | 1.29 | 1.24 | 1.24 | 1.29 |
| λ | 0.024 | 0.029 | 0.04 | 0.028 |
| κ | 0.01 | 0.01 | 0.01 | 0.01 |
| μ | 0.3 | 0.3 | 0.3 | 0.3 |
| Γ | 1.934 | 1.849 | 1.986 | 2.014 |
| n | 2 | 2 | 2 | 2 |
| r | 10 | 10 | 4 | 10 |

The correlation does depend on the soil type. For practical application, however, an average correlation may be useful (Figure 33). This is given below:

$$\frac{K_D}{K_0} = -185.4\xi_0^2 - 68.2\xi_0 + 7.3 \quad (64)$$

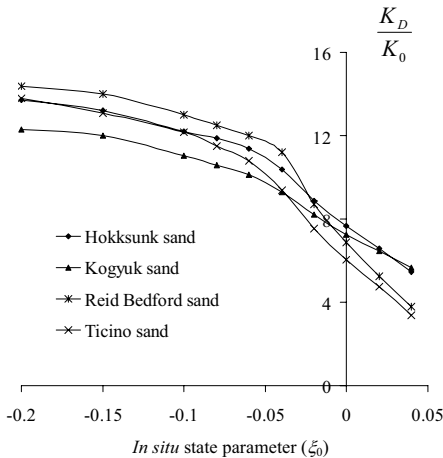


Figure 32: Theoretical correlations for deriving in situ state parameter

The numerical results are plotted in Figure 32 in terms of the normalised dilatometer horizontal index K_D/K_0 against the in situ state parameter ξ_0 prior to the dilatometer insertion. As expected, the normalised dilatometer horizontal index increases when the in situ state parameter decreases from a positive value (i.e., looser than critical state) to a negative value (i.e., denser than critical state).

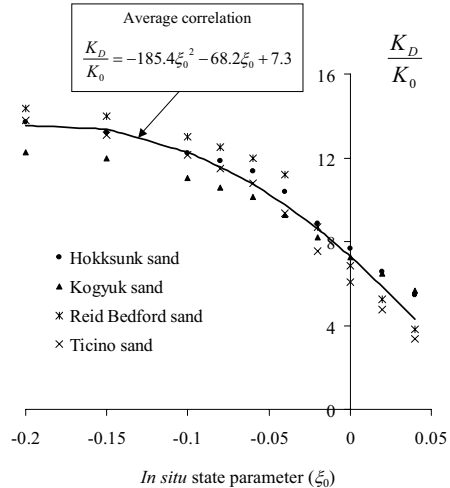


Figure 33: Average correlation for deriving in situ state parameter

Alternatively, the in situ state parameter may be estimated from the normalised dilatometer horizontal index using the following equation:

$$\xi_0 = -0.002 \left(\frac{K_D}{K_0} \right)^2 + 0.015 \left(\frac{K_D}{K_0} \right) + 0.0026 \quad (65)$$

9 PARTICLE MECHANICS APPROACH

9.1 Overview

So far almost all the analyses of in situ tests have been based on continuum mechanics by treating

soils as a continuous medium. A useful alternative, particularly for granular material, would be to treat it as a system of discrete particles. The theory of this approach is known as particle or discontinuous mechanics (Harr, 1977; Cundall and Strack, 1979). Application of this approach to the analysis of real soil mechanics problems is still limited because it requires a large number of particles to be used and therefore demands extensive computer resources.

9.2 DEM modelling of deep penetration in sand

Huang and Ma (1994) were among the first to apply the discrete element method (DEM) to simulate deep penetration in sand. In their study, a plane strain penetrometer was pushed into a ground made of a large number of particles. However, the number of simulations reported by them was very limited.

To gain further insights, a study using DEM to simulate deep wedge penetration in sand has been carried out most recently by Yu et al. (2004), who used a two-dimensional, plane strain DEM code that was an extended version of Jiang et al. (2003). The cohesionless soil chosen has a particle size distribution as shown in Figure 34. Due to the geometric

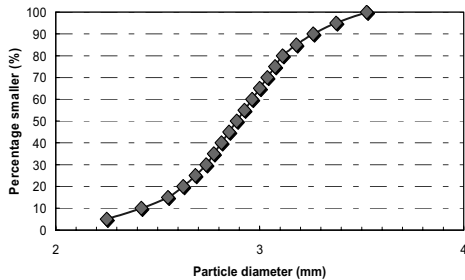


Figure 34: Particle size distribution of cohesionless soil

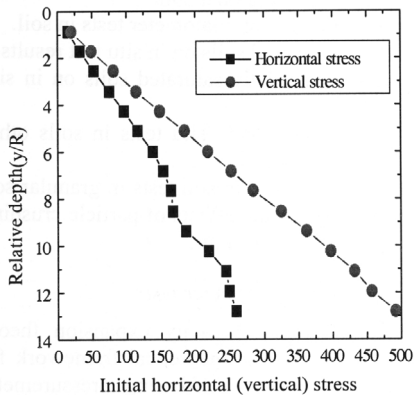


Figure 35: Initial stress state of cohesionless soil

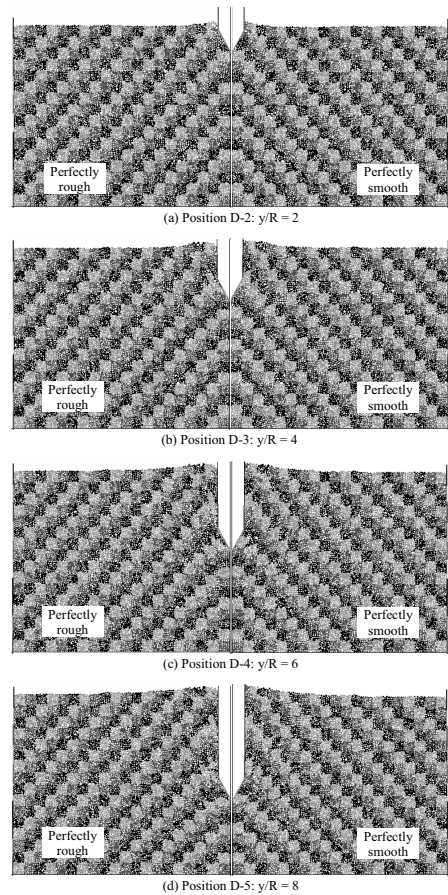


Figure 36: Process of deep penetration modelled by DEM

symmetry of the problem, only half of the medium-dense granular ground with a void ratio of 0.24 was considered. The penetrometer used in the simulations has a half-width of $R=18$ mm with an apex angle of 60° and is composed of 3 rigid walls, i.e. frictional tip wall, frictional and frictionless sleeve walls. A DEM-based simulation of deep penetration takes the following main steps:

- 1) A soil layer of 10,000 particles was first generated using the undercompaction method (Jiang et al. 2003) with depth and width as $16R$ and $17.5R$ respectively.
- 2) The soil layer was then allowed to settle under an amplified gravity field of $1000g$.
- 3) The top wall was removed to simulate a free boundary, and the remaining walls are kept as frictionless.
- 4) The outside boundary was divided into 10 small sections of the same height and the pressure on

each section was measured, and kept as a constant during the penetration to simulate a K_0 stress boundary condition, see Figure 35.

- 5) By choosing different values of the tip (sleeve)-particle friction, between 0 and 1.0, the penetrometer was pushed downward at 2 mm/s and several aspects of the test results were analysed.

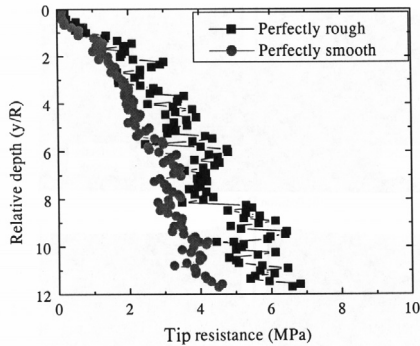


Figure 37: Penetration resistance versus penetration depth

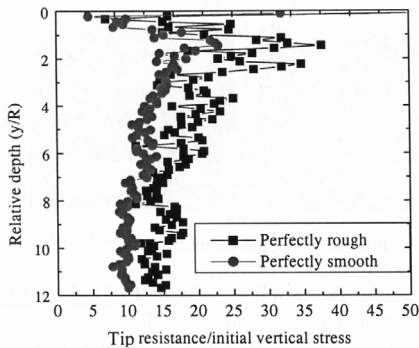


Figure 38: Normalised penetration resistance (cone factor) versus penetration depth

The continuous penetration process of a wedge penetrometer from the ground surface is shown in Figure 36 for both smooth and rough soil-penetrometer interfaces. As shown in Figure 37, the penetration resistance increases steadily with penetration depth and as expected a rough penetrometer generates a higher resistance. Plotted in Figure 38 are normalised penetration resistances (equivalent to the cone factor for cone penetrometers) against penetration depth. The pattern predicted with the discrete element method (DEM) is consistent with what was observed in both centrifuge testing of a cone penetrometer (Bolton et al., 1999) and calibration chamber testing of a plane strain pile (White,

2002) and a cone penetrometer (Houlsby and Hitchman, 1988).

10 CONCLUSIONS

10.1 Overview

The rational interpretation of in situ tests depends on the successful analysis of corresponding boundary value problems. As in the solution of most other soil mechanics and geotechnical engineering boundary value problems, continuum mechanics forms the main theoretical basis, although particle mechanics-based discrete element methods have the potential to further advance our understanding of in situ testing processes in granular soil.

Incomplete as this review had to be, the Author hopes that it has conveyed an idea of the tremendous development that has occurred in this field during the last two decades. In particular, significant progress has been made in developing the rational theoretical basis for the interpretation of pressuremeter tests in soils. Good progress has also been achieved in understanding the mechanics of cone penetration and dilatometer tests in undrained clay. These achievements justify the expectation that the next decade will see a more rapid development of mechanics-based, rigorous interpretation methods for in situ tests in some of the geomaterials that have so far proved intractable.

Mitchell et al. (1978) correctly pointed out that the refinement of existing procedures and further development of new methods of interpretation is an on-going process. Indeed, much research is still needed in further enhancing our understanding in the following key areas:

- 1) The mechanics of cone penetration/cone pressuremeter tests in granular soil.
- 2) The mechanics of flat dilatometer tests in soil.
- 3) The effect of layered soils on in situ test results.
- 4) The effect of partially saturated soils on in situ test results.
- 5) The interpretation of in situ tests in soils other than clay and sand.
- 6) The interpretation of in situ tests in granular soil by accounting for the effects of particle crushing and non-coaxial behaviour.

10.2 Self-boring pressuremeter tests

- 1) The one-dimensional cavity expansion theory proves to be a useful theoretical framework for the interpretation of self-boring pressuremeter tests.

- 2) The two-dimensional pressuremeter geometry effects appear to be significant but can be easily accounted for by applying the correction factors derived from finite element analysis.
- 3) The undrained condition assumed for tests in clay is valid only when the coefficient of permeability is less than 10^{-9} m/s.

10.3 Cone penetration/cone pressuremeter tests

- 1) The one-dimensional cavity expansion theory (applicable to both clay and sand) and the two-dimensional strain path method (applicable to undrained clay only at the present time) prove to be useful theoretical frameworks for the interpretation of cone penetration/cone pressuremeter tests.
- 2) The newly developed steady-state finite element technique and large strain finite element methods with adaptive remeshing are more general methods and potentially should provide a more accurate theoretical basis for the understanding of cone penetration/cone pressuremeter in soils.
- 3) The discrete element method (DEM) has the potential to be a useful theoretical tool for advancing our understanding of cone penetration/cone pressuremeter tests in granular soil.

10.4 Flat dilatometer tests

- 1) The two-dimensional flat cavity expansion method (applicable to both clay and sand) and the three-dimensional strain path method (applicable to undrained clay only at the present time) prove to be useful theoretical frameworks for modelling the installation of the flat dilatometer in soils.
- 2) The discrete element method (DEM) should provide a useful numerical tool for modelling the installation of a dilatometer into granular soils.
- 3) Other numerical techniques, such as three-dimensional finite element methods, will be required to model the expansion of the dilatometer following its insertion into the ground. No work of this type has been reported.

ACKNOWLEDGEMENTS

The Author is greatly honoured to have been selected by the Scientific Committee of ISC'2 (led by TC16 and TC10 of the International Society of Soil Mechanics and Geotechnical Engineering) to present the Inaugural James K. Mitchell Lecture. He is immensely privileged to have known and worked under Professor Mitchell, who is not only a giant of his

generation but also truly a teacher in the highest sense of the word.

The Author wishes to acknowledge support and contributions from many people during the preparation of this lecture: first and foremost his wife, Xiu-Li, daughter, Christina and son, Thomas for their encouragements and sacrifices; mentors at key stages of his career, Ted Brown, Peter Wroth, Jim Mitchell, Kerry Rowe and Steve Brown for their inspiration and guidance; colleagues and staff at the Nottingham Centre for Geomechanics (NCG), particularly Caroline Dolby, Glenn McDowell, Ed Ellis and Guoping Zhang, for their valuable assistance; collaborators, Guy Houlsby, Fernando Schnaid, John Carter, Ian Collins, Mark Randolph, Andrew Whittle, Len Herrmann, Ross Boulanger, Rodrigo Salgado, Ken Been, An-Bin Huang, and John Powell for many useful discussions; students and assistants of past and present including Rassoul Ajalloeian, Mark Charles, Cuong Khong, Xun Yuan, James Walker, Wenxiong Huang, and Mingjing Jiang for choosing to undertake research with him on in situ soil testing.

REFERENCES

- Abu-Farsakh, M., Tumay, M. and Voyiadjis, G. 2003. Numerical parametric study of piezocone penetration test in clays. *International Journal of Geomechanics*, 3(2):170-181.
- Ajalloeian, R. and Yu, H.S. 1998. Chamber studies of the effects of pressuremeter geometry on test results in sand. *Geotechnique*, 48(5): 621-636.
- Aubeny, C.P., Whittle, A.J. and Ladd, C.C. 2000. Effects of disturbance on undrained strengths interpreted from pressuremeter tests. *Journal of Geotechnical and Geoenvironmental Engineering*, ASCE, 126(12):1133-1144.
- Baguelin, F., Jezequel, J.F., Lemee, E. and Mehause, A. 1972. Expansion of cylindrical probe in cohesive soils. *Journal of the Soil Mechanics and Foundations Division*, ASCE, 98(11):1129-1142.
- Baligh, M.M. 1985. Strain path method. *Journal of Geotechnical Engineering*, ASCE, 111(3), 1108-1136.
- Baligh, M.M. 1986. Undrained deep penetration. I: shear stresses. *Geotechnique*, 36(4):471-485.
- Baligh, M.M and Levadoux, J.N. 1986. Consolidation after undrained piezocone penetration. II: Interpretation. *Journal of Geotechnical Engineering*, ASCE, 112(7):727-745.
- Been, K., Crooks, J.H.A., Becker, D.E. and Jefferies, M.G. 1987. The cone penetration test in sand: II general inference of state. *Geotechnique*, 37(3):285-299.
- Been, K. and Jefferies, M.G. 1985. A state parameter for sands. *Geotechnique*, 35(2):99-112.
- Bellotti, R., Ghionna, V., Jamiolkowski, M., Robertson, P.K. and Peterson, R.W. 1989. Interpretation of moduli from self-boring pressuremeter tests in sand. *Geotechnique*, 39(2):269-292.
- Bishop, R.F., Hill, R. and Mott, N.F. 1945. The theory of indentation and hardness tests. *Proceedings of Physics Society*, 57:147-159.
- Bolton, M.D. 1986. The strength and dilatancy of sands. *Geotechnique*, 36(1):65-78.

- Bolton, M.D., Gui, M.W., Garnier, J., Corte, J.F., Bagge, G., Laue, J. and Renzi, R. (1999). Centrifuge cone penetration tests in sand. *Geotechnique*, 49(4):543-552.
- Bolton, M.D. and Whittle, R.W. 1999. A non-linear elastic/perfectly plastic analysis for plane strain undrained expansion tests. *Geotechnique*, 49(1):133-141.
- Burland, J. 1989. Small is beautiful - the stiffness of soils at small strains. *Canadian Geotechnical Journal*, 26:499-516.
- Byrne, P.M., Salgado, F.M. and Howie, J.A. 1990. Relationship between the unload shear modulus from pressuremeter tests and the maximum shear modulus for sand. *Proceedings of ISP3*, Oxford, 231-241.
- Campanella, R.G. and Robertson, P.K. 1991. Use and interpretation of a research dilatometer. *Canadian Geotechnical Journal*, 28(1):113-126.
- Carter, J.P., Randolph, M.F. and Wroth, C.P. 1979. Stress and pore pressure changes in clay during and after the expansion of a cylindrical cavity. *International Journal for Numerical and Analytical Methods in Geomechanics*. 3:305-323.
- Cheng, J.H. 1988. Automatic adaptive remeshing for finite element simulation of forming processes. *International Journal for Numerical Methods in Engineering*, 26:1-18.
- Clarke, B.G., Carter, J.P. and Wroth, C.P. 1979. In situ determination of the consolidation characteristics of saturated clays. *Proceedings of 7th European Conference on Soil Mechanics*, Vol. 2:207-213.
- Collins, I.F. and Yu, H.S. 1996. Undrained cavity expansion in critical state soils. *International Journal for Numerical and Analytical Methods in Geomechanics*. 20(7):489-516.
- Collins, I.F., Pender, M.J. and Wang, Y. 1992. Cavity expansion in sands under drained loading conditions. *International Journal for Numerical and Analytical Methods in Geomechanics*, 16(1):3-23.
- Cudmani, R. and Osinov, V.A. (2001). The cavity expansion problem for the interpretation of cone penetration and pressuremeter tests. *Canadian Geotechnical Journal*, 38:622-638.
- Cundall, P.A. and Strack, O.D.L. 1979. A discrete numerical model for granular assemblies. *Geotechnique*, 29(1):47-65.
- Denby, G.M. and Clough, G.W. 1980. Self-boring pressuremeter tests in clay. *Journal of Geotechnical Engineering*, ASCE, 106(12):1369-1387.
- Durban, D. and Fleck, N.A. 1992. Singular plastic fields in steady penetration of a rigid cone. *Journal of Applied Mechanics*, ASME, 59:1725-1730.
- Durgunoglu, H.T. and Mitchell, J.K. 1975. Static penetration resistance of soils. *Proceedings of the ASCE Specialty Conference on In-Situ Measurements of Soil Properties*, Vol 1: 151-189.
- Fahey, M. and Carter, J.P. 1986. Some effects of rate of loading and drainage on pressuremeter tests in clays. *Proceedings of Speciality Geomechanics Symposium*, Adelaide, 50-55.
- Fahey, M. and Carter, J.P. 1993. A finite element study of the pressuremeter test in sand using a nonlinear elastic plastic model. *Canadian Geotechnical Journal*, 30:348-362.
- Ferreira, R.S. and Robertson, P.K. 1992. Interpretation of undrained self-boring pressuremeter test results incorporating unloading. *Canadian Geotechnical Journal*, 29:918-928.
- Finno, R.J. 1993. Analytical interpretation of dilatometer penetration through saturated cohesive soils. *Geotechnique*, 43(2):241-254.
- Fioravante, V., Jamiolkowski, M. and Lancellotta, R. 1994. An analysis of pressuremeter holding tests. *Geotechnique*, 44(2):227-238.
- Ghionna, V.N. and Jamiolkowski, M. 1991. A critical appraisal of calibration testing of sands. *Proceedings of 1st International Symposium on Calibration Chamber Testing*, Potsdam, 13-39.
- Gibson, R.E. and Anderson, W.F. 1961. In situ measurement of soil properties with the pressuremeter. *Civil Engineering Public Works Review*, Vol. 56:615-618.
- Hardin, B.O. 1978. The nature of stress-strain behaviour of soils. *Proceedings of ASCE Geotechnical Engineering Specialty Conference*, California, 3-90.
- Harr, M.E. 1977. *Mechanics of Particulate Media*. McGraw-Hill, New York.
- Hill, R. 1950. *The Mathematical Theory of Plasticity*. Oxford University Press.
- Hsieh, Y.M., Whittle, A.J. and Yu, H.S. 2002. Interpretation of pressuremeter tests in sand using advanced soil model. *Journal of Geotechnical and Geoenvironmental Engineering*, ASCE, 128(3):274-278.
- Houlsby, G.T. and Carter, J.P. 1993. The effect of pressuremeter geometry on the results of tests in clays. *Geotechnique*, 43:567-576.
- Houlsby, G.T. and Hitchman, R. 1988. Calibration chamber tests of a cone penetrometer in sand. *Geotechnique*, 38:575-587.
- Houlsby, G.T. and Withers, N.J. 1988. Analysis of the cone pressuremeter test in clay. *Geotechnique*, 38:575-587.
- Hu, Y. and Randolph, M.F. 1998. A practical numerical approach for large deformation problem in soil. *International Journal for Numerical and Analytical Methods in Geomechanics*, 22(5):327-350.
- Huang, A.B. 1989. Strain path analysis for arbitrary three dimensional penetrometers. *International Journal for Numerical and Analytical Methods in Geomechanics*.13:551-564.
- Huang, A.B. and Ma, M.Y. 1994. An analytical study of cone penetration tests in granular material. *Canadian Geotechnical Journal*, 31:91-103.
- Huang, W., Sheng, D., Sloan, S.W. and Yu, H.S. 2004. Finite element analysis of cone penetration in cohesionless soil. *Computers and Geotechnics* (accepted).
- Hughes, J.M.O., Wroth, C.P. and Windle, D. 1977. Pressuremeter tests in sands. *Geotechnique*, 27(4):455-477.
- Jamiolkowski, M. 1988. Research applied to geotechnical engineering. James Forrest Lecture. *Proceedings of Institution of Civil Engineers*, London, Part 1, 84:571-604.
- Jamiolkowski, M., Ladd, C.C., Germaine, J.T. and Lancellotta, R. 1985. New developments in field and laboratory testing of soils. Theme Lecture. *Proceedings of the 11th International Conference on Soil Mechanics and Foundation Engineering*, Vol 1:57-154.
- Jang, I.S., Chung, C.K., Kim, M.M. and Cho, S.M. 2003. Numerical assessment on the consolidation characteristics of clays from strain holding, self-boring pressuremeter test. *Computers and Geotechnics*, 30:121-140.
- Jardine, R.J. 1992. Nonlinear stiffness parameters from undrained pressuremeter tests. *Canadian Geotechnical Journal*, 29(3):436-447.
- Jefferies, M.G. 1988. Determination of horizontal geostatic stress in clay with self-bored pressuremeter. *Canadian Geotechnical Journal*, 25:559-573.
- Jiang, M.J., Konrad, J.M. and Leroueil, S. 2003. An efficient technique for generating homogeneous specimens for DEM studies. *Computers and Geotechnics*, 30(7):579-597.
- Konrad, J.M. 1998. Sand state from cone penetrometer tests: a framework considering grain crushing stress. *Geotechnique*, 48(2):201-215.

- Ladanyi, B. 1972. In situ determination of undrained stress-strain behaviour of sensitive clays with the pressuremeter. *Canadian Geotechnical Journal*, 9(3):313-319.
- Ladanyi, B. and Johnston, G.H. 1974. Behaviour of circular footings and plate anchors embedded in permafrost. *Canadian Geotechnical Journal*, 11:531-553.
- Ladd, C.C., Foott, R., Ishihara, K., Schlosser, F. and Poulos, H.G. 1977. Stress-dormation and strength characteristics. Theme Lecture. *Proceedings of 9th International Conference on Soil Mechanics and Foundation Engineering*. Vol.2:421-497.
- Lee, N.S. and Bathe, K.J. 1994. Error indicators and adaptive remeshing in large deformation finite element analysis. *Finite Element Analysis in Design*, 16:99-139.
- Levadoux, J.N. and Baligh, M.M. 1986. Consolidation after undrained piezocone penetration. I: prediction. *Journal of Geotechnical Engineering*, ASCE, 112(7):707-726.
- Lu, Q. 2004. *A Numerical Study of Penetration Resistance in Clay*. PhD Thesis, The University of Western Australia.
- Lunne, T., Robertson, P.K. and Powell, J.J.M. 1997. *Cone Penetration Testing*. E&FN Spon, London.
- Lutenegger, A.J. 1988. Current status of the Marchetti dilatometer test. Special Lecture. *Proceedings of 1st International Symposium on Penetration Testing (ISOPT-1)*, Orlando, 1:137-155.
- Lutenegger, A.J., Blanchard, J.D. (1990). A comparison between full displacement pressuremeter tests and dilatometer tests in clay., *Proceedings of ISP3*, Oxford, 309-320.
- Mair, R.J. and Wood, D.M. 1987. *Pressuremeter Testing, Methods and Interpretation*. CIRIA Report, Butterworths, London.
- Manassero, M. 1989. Stress-strain relationships from drained self-boring pressuremeter tests in sand. *Geotechnique*, 39(2):293-308.
- Marchetti, S. 1980. In situ tests by flat dilatometer. *Journal of Geotechnical Engineering*, ASCE, 106(GT3):299-321.
- Marchetti, S, Monaco, P., Totani, G. and Calabrese, M. 2001. The flat dilatometer test (DMT) in soil investigations. *A Report by the ISSMGE Committee TC 16. Proceedings of International Conference on In situ Measurement of Soil Properties*, Bali, 41pp.
- Mayne, P.W. 1993. In situ determination of clay stress history by piezocone. In: *Predictive Soil Mechanics*, Thomas Telford, London, 483-495.
- Mayne, P.W. and Kulhawy, F.H. 1982. K_0 -OCR relationships in soils. *Journal of Geotechnical Engineering*, ASCE, 108(6):851-872.
- Mayne, P.W. and Martin, G.K.1998. Commentary on Marchetti flat dilatometer correlations in soils. *ASTM Geotechnical Testing Journal*, 21(3):222-239.
- McDowell, G.R. and Bolton, M.D. 1998. On the micromechanics of crushable aggregates. *Geotechnique*, 48(5):667-679.
- Mitchell, J.K. and Brandon, T.L. 1998. Analysis and use of CPT in earthquake and environmental engineering. Keynote Lecture, *Proceedings of ISC'98*, Vol.1:69-97.
- Mitchell, J.K., Guzikowski, F. and Villet, W.C.B. 1978. The measurement of soil properties in-situ: present methods – their applicability and potential. *Lawrence Berkeley Laboratory Report 6363*, University of California at Berkeley.
- Mitchell, J.K. and Keaveny, J.M. 1986. Determining sand strength by cone penetrometer. *Proceedings of the ASCE Specialty Conference, In Situ'86*, Blacksburg, 823-839.
- Morrison, J.L.M. 1948. The criterion of yield of Gun steel. *Proceedings of the Institution of Mechanical Engineers*, 159:81-94.
- Palmer, A.C. 1972. Undrained plane strain expansion of a cylindrical cavity in clay: a simple interpretation of the pressuremeter test. *Geotechnique*, 22(3):451-457.
- Parkin, A.K. and Lunne, T. 1982. Boundary effects in the laboratory calibration of a cone penetrometer in sand. *Proceedings of 2nd European Symposium on Penetration Testing*, Amsterdam, 2:761-768.
- Powell, J.J.M. 2004. Personal communication.
- Powell, J.J.M. and Shields, C.H. 1997. The cone pressuremeter - a study of its interpretation in Holmen sand. *Proceedings of 14th International Conference on Soil Mechanics and Foundation Engineering*, 573-576.
- Powell, J.J.M. and Uglow, I.M. 1988. The interpretation of the Marchetti dilatometer test in UK clays. *Proceedings of Penetration Testing in the UK*, Thomas Telford, Paper 34:269-273.
- Prapaharan, S., Chameau, J.L. and Holtz, R.D. 1989. Effect of strain rate on undrained strength derived from pressuremeter tests. *Geotechnique*, 39(4):615-624
- Prevost, J.H. and Hoeg, K. 1975. Analysis of pressuremeter in strain softening soil. *Journal of Geotechnical Engineering*, ASCE, Vol. 101(GT8):717-732.
- Pyrah, I.C. and Anderson, W.F. 1990. Numerical assessment of self-boring pressuremeter tests in a clay calibration chamber. *Proceedings of ISP3*, 179-188.
- Randolph, M.F. and Wroth, C.P. 1979. An analytical solution for the consolidation around a driven pile. *International Journal for Numerical and Analytical Methods in Geomechanics*, 3:217-229.
- Robertson, P.K. 1986. In situ testing and its application to foundation engineering. *Canadian Geotechnical Journal*, 23(4):573-594.
- Robertson, P.K., Sully, J.P., Woeller, D.J., Luune, T., Powell, J.J.M. and Gillespie, D.G. 1992. Estimating coefficient of consolidation from piezocone tests. *Canadian Geotechnical Journal*, 29(4):551-557.
- Robertson, P.K. et al. 2000. The Canadian Liquefaction Experiment: an overview. *Canadian Geotechnical Journal*, 37:499-504.
- Russell, A.R. and Khalili, N. 2002. Drained cavity expansion in sands exhibiting particle crushing. *International Journal for Numerical and Analytical Methods in Geomechanics*, 26:323-340.
- Sagaseta, C. and Houlsby, G.T. 1992. Stresses near the shoulder of a cone penetrometer in clay. *Proceedings of 3rd International Conference on Computational Plasticity*, Vol.2:895-906.
- Salgado, R. 1993. *Analysis of Penetration Resistance in Sands*. PhD Thesis, University of California at Berkeley.
- Salgado, R., Mitchell, J.K. and Jamiolkowski, M. 1997. Cavity expansion and penetration resistance in sand. *Journal of Geotechnical and Geoenvironmental Engineering*, ASCE, 123(4):344-354.
- Schnaid, F. 1990. *A Study of the Cone Pressuremeter Test in Sand*. DPhil Thesis, Oxford University.
- Silvestri, V. 2001. Interpretation of pressuremeter tests in sand. *Canadian Geotechnical Journal*, 38:1155-1165.
- Sladen, J.A. 1989. Problems with interpretation of sand state from cone penetration test. *Geotechnique*, 39(2):323-332.
- Smith, M.G. and Houlsby, G.T. 1995. Interpretation of the Marchetti dilatometer in clay. *Proceedings of 11th ECSMFE*, Vol 1:247-252.
- Sousa Coutinho, A.G.F. 1990. Radial expansion of cylindrical cavities in sandy soils: application to pressuremeter tests. *Canadian Geotechnical Journal*, 27:737-748.
- Su, S.F. and Liao, H.J. 2002. Influence of strength anisotropy on piezocone resistance in clay. *Journal of Geotechnical*

- and *Geoenvironmental Engineering*, ASCE, 128(2):166-173.
- Teh, C.I. and Houlsby, G.T. 1991. An analytical study of the cone penetration test in clay. *Geotechnique*, 41(1):17-34.
- Torstensson, B.A. 1977. The pore pressure probe. Norskjording- og fjellteknisk forbund. Fjellsprengningsteknikk – bergmekanikk – geoteknikk, Oslo, Foredrag, 34.1-34.15, Trondheim, Norway, Tapir.
- Van den Berg, P. 1994. *Analysis of Soil Penetration*, PhD Thesis, Delft University.
- Vesic, A.S. 1977. Design of pile foundations. *National Cooperation Highway Research Program, Synthesis of Highway Practice* 42. TRB, National Research Council, Washington DC.
- White, D.J. 2002. *An Investigation Into Behaviour of Pressed-in Piles*. PhD Thesis, Cambridge University.
- Whittle, A.J. and Aubeny, C.P. 1993. The effects of installation disturbance on interpretation of in situ tests in clays. In: *Predictive Soil Mechanics*, Thomas Telford, London, 742-767.
- Withers, N.J., Howie, J, Hughes, J.M.O. and Robertson, P.K. 1989. Performance and analysis of cone pressuremeter tests in sands. *Geotechnique*, 39(3):433-454.
- Wood, D.M. 1990. *Soil Behaviour and Critical State Soil Mechanics*, Cambridge University Press.
- Wroth, C.P. 1982. British experience with the self-boring pressuremeter. *Proceedings of the Symposium o Pressuremeter and its Marine Applications*, Paris, Editions Technip, 143-164.
- Wroth, C.P. 1984. The interpretation of in situ soil tests. *Geotechnique*, 34:449-489.
- Wroth, C.P. and Bassett, N. 1965. A stress-strain relationship for the shearing behaviour of sand. *Geotechnique*, 15(1):32-56.
- Wroth, C.P. and Houlsby, G.T. 1985. Soil mechanics – property characterization and analysis procedures. Theme Lecture No. 1. *Proceedings of 11th International Conference on Soil Mechanics and Foundation Engineering*. Vol 1:1-56.
- Wroth, C.P. and Hughes, J.M.O. 1972. An instrument for the in situ measurement of the properties of soft clays. *Report CUED/D, Soils TR13*. University of Cambridge.
- Wroth, C.P., Randolph, M.F., Houlsby, G.T. and Fahey, M. 1979. A review of the engineering properties of soils with particular reference to the shear modulus. *Cambridge University Report CUED/D Soils TR75*.
- Yeung, S.K. and Carter, J.P. 1990. Interpretation of the pressuremeter test in clay allowing for membrane end effects and material non-homogeneity. *Proceedings of 3rd International Symposium on Pressuremeters*, Oxford, 199-208.
- Yu, H.S. 1990. *Cavity Expansion Theory and its Application to the Analysis of Pressuremeters*. DPhil Thesis, Oxford University.
- Yu, H.S. 1993a. A new procedure for obtaining design parameters from pressuremeter tests. *Australian Civil Engineering Transactions*, Vol. CE35 (4):353-359.
- Yu, H.S. 1993b. Discussion on: singular plastic fields in steady penetration of a rigid cone. *Journal of Applied Mechanics*, ASME, 60:1061-1062.
- Yu, H.S. 1994. State parameter from self-boring pressuremeter tests in sand. *Journal of Geotechnical Engineering*, ASCE, 120(12):2118-2135.
- Yu, H.S. 1996. Interpretation of pressuremeter unloading tests in sands. *Geotechnique*, 46(1):17-31.
- Yu, H.S. 1998. CASM: A unified state parameter model for clay and sand. *International Journal for Numerical and Analytical Methods in Geomechanics*, 22:621-653.
- Yu, H.S. 2000. *Cavity Expansion Methods in Geomechanics*. Kluwer Academic Publishers, The Netherlands.
- Yu, H.S. and Carter, J.P. 2002. Rigorous similarity solutions for cavity expansion in cohesive-frictional soils. *International Journal of Geomechanics*, 2(2):233-258.
- Yu, H.S., Carter, J.P. and Booker, J.R. 1993. Analysis of the dilatometer test in undrained clay. In: *Predictive Soil Mechanics*, Thomas Telford, London, 783-795.
- Yu, H.S., Charles, M. and Khong, C.D. 2003. Analysis of pressuremeter geometry effects using critical state models. *International Journal for Numerical and Analytical Methods in Geomechanics* (under review).
- Yu, H.S. and Collins, I.F. 1998. Analysis of self-boring pressuremeter tests in overconsolidated clays. *Geotechnique*, 48(5):689-693.
- Yu, H.S., Herrmann, L.R. and Boulanger, R.W. 2000. Analysis of steady cone penetration in clay. *Journal of Geotechnical and Geoenvironmental Engineering*, ASCE, 126(7):594-605.
- Yu, H.S. and Houlsby, G.T. 1991. Finite cavity expansion in dilatant soil: loading analysis. *Geotechnique*, 41(2):173-183.
- Yu, H.S. and Houlsby, G.T. 1995. A large strain analytical solution for cavity contraction in dilatant soils. *International Journal for Numerical and Analytical Methods in Geomechanics*, 19(11):793-811.
- Yu, H.S., Jiang, M. and Harris, D. 2004. DEM simulation of deep penetration in granular soil. *Journal of Geotechnical and Geoenvironmental Engineering*, ASCE (under review).
- Yu, H.S. and Mitchell, J.K. 1996. Analysis of cone resistance: a review of methods. *Research Report No. 142.09.1996*, The University of Newcastle, NSW, 50pp.
- Yu, H.S. and Mitchell, J.K. 1998. Analysis of cone resistance: review of methods. *Journal of Geotechnical and Geoenvironmental Engineering*, ASCE, 124(2):140-149.
- Yu, H.S., Schnaid, F. and Collins, I.F. 1996. Analysis of cone pressuremeter tests in sand. *Journal of Geotechnical Engineering*, ASCE, 122(8):623-632.
- Yu, H.S. and Whittle, A.J. 1999. Combining strain path analysis and cavity expansion theory to estimate cone resistance in clay. *Unpublished Notes*.
- Yu, P. and Richart, F.E. 1984. Stress ratio effects on shear moduli of dry sands. *Journal of Geotechnical Engineering*, ASCE, 110(3):331-345.